Journal of Chromatography, 300 (1984) 165–223
Chromatographic Reviews
Elsevier Science Publishers B.V., Amsterdam — Printed in The Netherlands

CHREV. 176

ISOELECTRIC FOCUSING IN IMMOBILIZED pH GRADIENTS

PIER GIORGIO RIGHETTI
Chair of Biochemistry, Faculty of Pharmaceutical Sciences and Department of Biomedical Sciences and Technologies, University of Milan, Via Celoria 2, Milan 20133 (Italy)
(Received December 5th, 1983)

CONTENTS

0378-4355/84/$17.70

The man that was used up.
A tale of the late Bugaboo and Kickapoo campaign
Edgar Allan Poe[1]

1. INTRODUCTION

To be frank, I thought that present day isoelectric focusing (IEF), just like Brevet Brigadier General John A. B. C. Smith, the hero of the above tale from Poe, had been totally spent and only ashes and few spare parts lay scattered on the ground. I feel so ashamed about it, that I don't think I am entitled to tell you this new story. Therefore, I will ask some characters from Poe's novel, the most reverend Doctor Drummummupp and my two girl friends, those exquisite specimens of affability and omniscience, the Misses Arabella and Miranda Cognoscenti, to introduce you to this new field on my behalf.

Fig. 1 gives the Darwinian evolutionary pathway of the concept of IEF. Born "artificially" with Kolin[2], it grew and aged "naturally" with Svensson-Rilbe[3], to be re-born "artificially yet naturally"[4], in a Pindaric flight that allowed us to close the

THE EVOLUTION OF THE CONCEPT OF ISOELECTRIC FOCUSING

1) ARTIFICIAL pH GRADIENTS:
DIFFUSION OF NON-AMPHOTERIC BUFFERS IN AN ELECTRIC FIELD
A. KOLIN (1955) PRC. NATL. ACAD. SCI. U.S., 41, 101-110

2) NATURAL pH GRADIENTS:
ELECTRIC TRANSPORT OF A MULTITUDE OF AMPHOTERIC, "CARRIER" BUFFERS
H. SVENSSON-RILBE (1962) ACTA CHEM. SCAND. 16, 456-466

3) ARTIFICIAL-YET-NATURAL pH GRADIENTS (IMMOBILIZED pH GRADIENTS):
NON-AMPHOTERIC BUFFERS GRAFTED TO A MATRIX
B. BJELLQVIST, K. EK, P.G. RIGHETTI, E. GIANAZZA, A. GÖRG, W. POSTEL
& R. WESTERMEIER (1982) J. BIOCHEM. BIOPHYS. METHODS 6, 317-339

Fig. 1. Darwinian evolution pathway of the concept of isoelectric focusing.

circle. This last statement, although antithetic, can be explained in the following way: (1) immobilized pH gradients (IPGs) appear to be artificial because they have the basic characteristics of Kolin's gradients, i.e., (a) the buffers are non-amphoteric; and (b) the pH gradient pre-exists before the application of the electric field; (2) however, IPGs are even more natural than Svensson-Rilbe's gradients because (a) they are truly indefinitely stable; and (b) they allow for a "natural" milieu in which the proteins will focus, *i.e.*, the ideal ionic strength and just the required buffering capacity.

Why was it necessary to resort to IPGs? Conventional IEF, the 23-year-old pupil of Svensson-Rilbe, had begun to show the crippling diseases of age, such as (a) instability of pH gradients with time (cathodic drift)[5]; (b) lack of even conductivity and buffering capacity[6]; (c) extremely low and unknown ionic strength[7]; and (d) limited load capacity, mostly due to isoelectric precipitation caused by the low ionic strength environment[8]. Grafted pH gradients, as the reader will appreciate, have completely solved all these problems.

2. THE IMMOBILINE SYSTEM

This section will deal with the properties of the new buffers and of the matrix used to insolubilize the pH gradients. As such, the concept of insolubilizing biological molecules is not completely new: it started in the late 1960s with immobilization on to granulated supports of specific protein ligands (affinity chromatography)[9], then of proteins themselves (insoluble enzymes)[10] and finally even of cells and microorganisms[11]. However, the concept of grafting to a porous support an entire pH gradient, thus forcing a proton field to be permanently bound to such a matrix, is novel and revolutionary. For those who desire to start the game of the "defocusing of the origin of ideas"[12], I could quote Martin and Hampson[13], who have used amphoteric, isoelectric membranes in the separation process named "steady-state rheoelectrolysis" by Rilbe[14], but this bears only a very faint resemblance, if any, to our method. I am now forced to quote the Japanese[15], who have bravely reported the possibility of grafting isoelectric carrier ampholytes to a support: however, their research does not seem to have progressed much beyond the pictogram of Fig. 2. I must confess that my group in Milan has worked extensively on this latter aspect (E. Gianazza, O. Brenna and P. G. Righetti, unpublished work), only to come to the conclusions that this is a dead end: it will not solve the problems of conventional IEF, but will surely aggravate them. Thus I can confidently repeat that present-day IPGs represent a really novel and revolutionary technique.

2.1. The chemicals

IPGs are based on the principle that the pH gradient, which exists prior to the IEF run itself, is copolymerized, and thus insolubilized, within the fibres of the polyacrylamide matrix. This is achieved by using, as buffers, a set of seven chemicals (called Immobiline, by analogy with Ampholine) whose pK values and physico-chemical data are given in Table 1. These compounds are acrylamide derivatives with the general structure

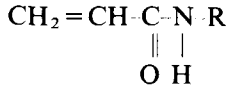

TABLE 1

PROPERTIES OF IMMOBILINES

From Bjellqvist *et al.*; see ref. 4.

Immobiline	*Apparent pK values* ($I = 10^{-2}$)*						
	H_2O		*Polyacrylamide gel** (T = 5%, C = 3%)*		*Polyacrylamide gel** [T = 5%, C = 3%; glycerol = 25% (w/v)]*		*Physical state at room temperature*
	10°C	*25°C*	*10°C*	*25°C*	*10°C*	*25°C*	
Acids with carboxyl as buffering group:							
p*K* 3.6	3.57	3.58	–	–	3.68 ± 0.02	3.75 ± 0.02	Solid
p*K* 4.4	4.39	4.39	4.30 ± 0.02	4.36 ± 0.02	4.40 ± 0.03	4.47 ± 0.03	Solid
p*K* 4.6	4.60	4.61	4.51 ± 0.02	4.61 ± 0.02	4.61 ± 0.02	4.71 ± 0.03	Solid
Bases with tertiary amine as buffering group:							
p*K* 6.2	6.41	6.23	6.21 ± 0.05	6.15 ± 0.03	6.32 ± 0.08	6.24 ± 0.07	Solid
p*K* 7.0	7.12	6.97	7.06 ± 0.07	6.96 ± 0.05	7.08 ± 0.07	6.95 ± 0.06	Solid
p*K* 8.5	8.96	8.53	8.50 ± 0.06	8.38 ± 0.06	8.66 ± 0.09	8.45 ± 0.07	Liquid
p*K* 9.3	9.64	9.28	9.59 ± 0.08	9.31 ± 0.07	9.57 ± 0.06	9.30 ± 0.05	Liquid

* p*K* values measured with glass surface electrode given without any corrections.

** Mean values of 10 determinations. Owing to the slow response of the electrode the p*K* values for the amines are uncertain.

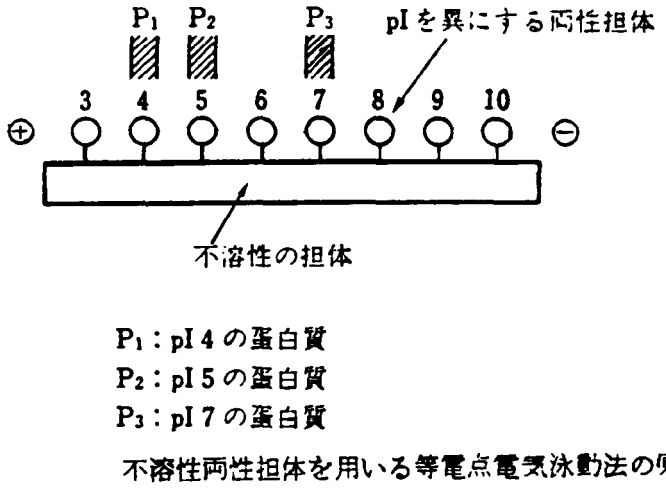

Fig. 2. A possible (mis)interpretation: isoelectric carrier ampholytes (p*I* 3, 4, 5, etc.) grafted to a support. Prizes will be given to any non-Japanese able to clarify the message (from Matuo *et al.*; see ref. 15).

where R contains either a carboxyl or a tertiary amino group. During gel polymerization, these buffering species are efficiently incorporated into the gel. The distance between the double bond and the group taking part in the protolytic equilibrium has in all instances been chosen to be long enough for the influence of the double bond on the dissociation constant to be neglected. As a result, the pK difference between the free and bound Immobiline is mainly due to the presence of the polyacrylamide matrix and to temperature variations during the IEF run. Immobiline-based pH gradients can be cast in the same way as a conventional polyacrylamide gradient gel, by using a density gradient to stabilize the Immobiline concentration gradient, with the aid of a standard, two-vessel gradient mixer (see Methodology). As shown in the formula, these buffers are no longer amphoteric, as in conventional IEF, but are bifunctional: at one extreme of the molecule is located the buffering group, and at the other extreme is the acrylic double bond, which will be consumed during the grafting process.

Fig. 3 gives the temperature coefficients (dpK/dT) for the seven Immobiline species in the temperature range 10–25°C. In agreement with their known chemical composition, it can be seen that the three carboxylic compounds, which are known to have in general very small standard heats of ionization (*ca.* 1 kcal/mol), exhibit negligible pK variations in this temperature range. On the other hand, the four tertiary amino derivatives, which are known to have larger standard heats of ionization (6–14 kcal/mol)[17] exhibit progressively increasing ΔpK values in this temperature range (the largest one, ΔpK = 0.44, corresponding to Immobiline of pK 8.5) (in connection with this, it should be stated that conventional carrier ampholytes, being composed of carboxyl and amino groups, exhibit similar temperature dependences of their pKs). Therefore, for reproducible runs and pH gradient calculations, all the experimental parameters have been fixed at 10°C[4]. Temperature is not the only variable that will affect Immobiline pKs (and therefore the actual pH gradient generated): additives in the gel that will change the water structure (chaotropic agents, such as

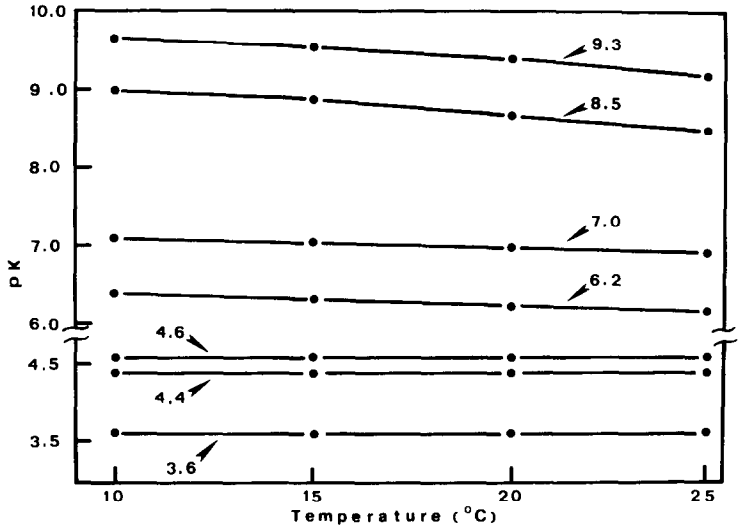

Fig. 3. Temperature coefficients (dpK/dT) for the seven Immobiline chemicals in the temperature range 10 25°C (from Righetti *et al.*; see ref. 16).

urea) or will lower its dielectric constant, and the ionic strength itself of the solution, will alter their pK values: for the corrections to be made, see Section 4.11.

What exactly the R group is in the Immobiline formula given above is a well guarded commercial secret; at a recent seminar which I attended in Osaka, my friend Takekazu Horio gave all the formulae as resolved by NMR, but as I am very poor at taking notes in Japanese I am afraid you will have to wait for him to publish a (Japanese?) paper on them. As a curiosity, we have taken these chemicals, subjected them to standard hydrolysis for proteins (azeotropic HCl, 24 h, 110°C, nitrogen atmosphere) and run them through the amino acid autoanalyser; as shown in Fig. 4, four peaks appear in the eluate, obscuring the following peaks: alanine (pK 3.6), tyrosine (pK 4.4 and 4.6) and ammonia (pK 6.2). Thus, it does not pay to have a peptide or protein peak, recovered from an Immobiline matrix, contaminated by these chemicals[7]. The list of compounds in Table 1 is not exhaustive: although at present there are only seven species, for generation of extended pH gradients, with a two-chamber mixer, you will need two additional ones: a strongly acidic (pK < 1) and a strongly basic (pK = 14) compound with pKs well outside the desired pH range. It is not unreasonable to predict that they will contain a sulphate and a quaternary amino group, respectively.

2.2. The Immobiline matrix

Fig. 5 depicts a segment of a hypothetical structure of an Immobiline matrix (lower tracing) as compared with the partial formula of a carrier ampholyte molecule (in the former, the long strings represent the polyacrylamide coils, while the short, vertical segments are the cross-links). Being copolymerized within the matrix, the Immobiline buffers cannot migrate any longer in the electric field: this means that the pH gradient is indefinitely stable (but it has to pre-exist before the onset of

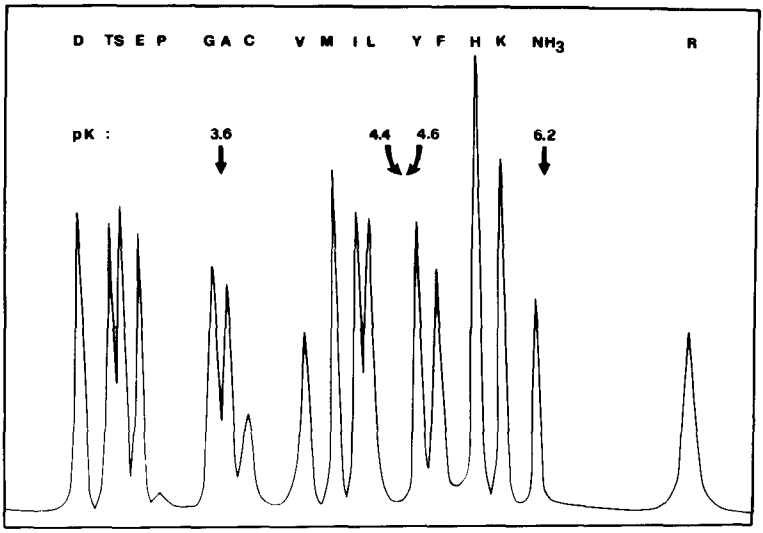

Fig. 4. Interference from Immobilines in amino acid analysis. A sample of each Immobiline was hydrolysed and run on an ion-exchange automatic chromatograph for amino acid analysis. The elution profiles of their split products are shown by arrows on a typical chromatogram of natural amino acids, which are identified by their one-letter symbols in the top row (from Gianazza *et al.*; see ref. 18).

polymerization) and can only be destroyed if and when the polyacrylamide gel is hydrolysed.

At the matrix concentration normally used (5% T*) and at the standard Immobiline levels (*ca.* 10 m*M* buffering ion) there is about one buffering group (or titrant) every 75 acrylamide residues, which means that, statistically, there are about 150 carbon atoms between two adjacent Immobiline species. This is extremely important for the ionic strength of the system, as compared with conventional IEF (see

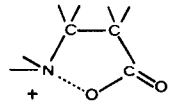

Ampholine

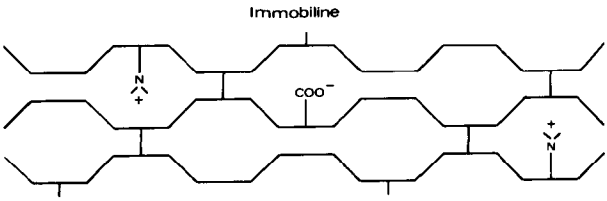

Fig. 5. Comparison between ionic strength in Ampholine and Immobiline gels. The upper drawing depicts a segment of an isoelectric Ampholine molecule, and the lower tracing shows a portion of an Immobiline gel. An Ampholine molecule, at its p*I*, is likely to form an inner salt, which does not contribute to the ionic strength of the system. The fixed charges in the Immobiline gel, being spaced *ca.* 150 carbon atoms apart, are believed to behave as point charges in the surrounding space, thus effectively contributing to the ionic strength of the milieu (from Righetti *et al.*; see ref. 16).

* T = (g acrylamide + g Bis)/100 ml solution); C = g Bis/% T.

also Section 5.2). We have also tried other cross-linkers (DHEBA, BAC, Acrylaide), but it seems that nothing matches the couple acrylamide–Bis in terms of polymerization efficiency (Gelfi and Righetti[19] and unpublished work). We have also tried gels with lower %T[20]: these softer gels (in the range 2.5–3% T) have a greatly increased loading capacity for preparative runs, as they give sharper bands, possibly owing to the local increase in charge density in the polyacrylamide matrix. Therefore, even for analytical experiments, we recommend diluted gels, such as 3.5% T (see also Section 5.6). However, even the most diluted matrices do not exhibit a substantial increase in pore size, so that large molecules (above 0.5×10^6 daltons) have great difficulty in migrating in IPG gels; at present, this is one of the major limitations of the IPG technique, which we have been unable to master either by drastically lowering %T or by greatly increasing %C (Gelfi and Righetti, unpublished work).

2.3. Comparison between Immobiline and Ampholine gradients

Fig. 6 lists the advantages and drawbacks of IPGs. Among the advantages are the following:

(a) increased resolution, due to the possibility of casting very shallow pH gradients (as narrow as 0.1 pH unit);

(b) unlimited stability, due to the fact that the buffers are grafted to the matrix (abolition of cathodic drift);

IMMOBILINE™ GRADIENTS VS. CARRIER AMPHOLYTE GRADIENTS

ADVANTAGES	DISADVANTAGES
o INCREASED RESOLUTION	o LONGER FOCUSING TIME
o UNLIMITED STABILITY	o GEL PREPARATION MORE TIME CONSUMING
o UNSENSITIVE TO DISTURBANCES (NO DISTORTED PROTEIN ZONES)	
o INCREASED LOADING CAPACITY	
o GIVES FULL FREEDOM IN THE CHOICE OF pH GRADIENT WIDTH AND SLOPE	
o BETTER REPRODUCIBILITY	
o FULL CONTROL OF pH, BUFFERING CAPACITY AND IONIC STRENGTH	
o IN PREPARATIVE WORK NO PROBLEMS SEPARATING SAMPLE FROM BUFFER	

Fig. 6. Comparison between Immobiline and Ampholine pH gradients (courtesy of Dr. B. Bjellqvist).

(c) insensitivity to salt and buffer disturbances from the sample; this results in undistorted protein bands (no more wavy zones);

(d) increased load capacity (as seen in Section 5.1, a 10-fold increase over carrier ampholyte gels);

(e) flexibility in the choice of any pH interval and any pH slope desired for any given separation problem;

(f) higher reproducibility than in carrier ampholyte (CA) gels, as the desired pH interval is mathematically formulated and fixed during the run;

(g) complete control of the important experimental parameters: pH interval and slope, buffering capacity (β) and ionic strength (I);

(h) possibility of running high sample volumes, in preparative work, without a prior dialysis step.

The disadvantages include the following:

(1) longer focusing times (but with the 5 kV power supply, the Macrodrive, and in wide pH gradients, >3 pH unit, the running times are greatly reduced;

(2) gel casting is more complex than in CA gels, but just as complex as preparing an O'Farrell gel[21].

3. THEORY

I shall review in this section the basic theory underlying the generation of immobilized pH gradients, in narrow and ultra-narrow ranges as well as in extended pH intervals. For the generation of reproducible pH gradients suitable for IEF in IPGs, the following criteria have to be met: (a) the pH gradient should be linear; (b) the buffering capacity (β) should be sufficiently high to render the pH gradient insensitive to impurities and to some inaccuracy in the preparation of the starting solutions (*e.g.*, acrylic acid in the acrylamide stock solution); (c) the β power should be as constant as possible in order to minimize deviations from linearity of the desired pH gradient and to reduce the effect of small disturbances in the gel mixing and casting on the generated pH gradient.

3.1. Narrow and ultra-narrow pH gradients

3.1.1. The principle of an Immobiline gradient

When casting a narrow Immobiline gradient, only a single buffering species is used and is titrated around its pK value with another, fully dissociated Immobiline. Why, then, is a linear pH gradient obtained as shown in Fig. 7?: any weak acid or base, when titrated around its pK, will automatically generate a linear pH gradient, which corresponds to a portion of its titration curve, centred on pH = pK. Fig. 7 shows the titration of Immobiline of pK 7.0, at constant concentration in solution, with 0.1 N hydrochloric acid. The free base, in solution, will give an alkaline pH; on addition of the first few drops of hydrochloric acid, the pH decays exponentially and then linearly in the pH interval (pK + 0.5 pH unit) to (pK − 0.5 pH unit). Below the lower limit, the pH drops dramatically to the pH produced by the excess of free hydrochloric acid at a given concentration, in solution. So, by titrating any Immobiline chemical in a pH interval no greater than 1 pH unit, centred on its pK, we can automatically generate any linear pH gradient in the pH range 3.5–9.5.

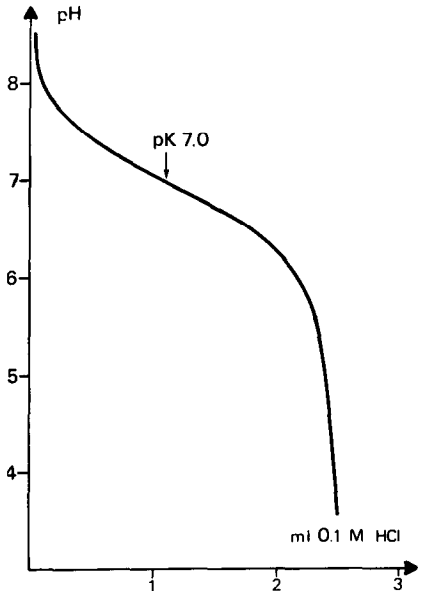

Fig. 7. Titration of pK 7.0 Immobiline with 0.1 M hydrochloric acid. If the buffering Immobiline concentration is kept constant, the titration curve produces a linear pH gradient around the pK (courtesy of Dr. B. Bjellqvist).

3.1.2. The Henderson–Hasselbach (H–H) equation

The random distribution of Immobilines within the gel fibres means that the protolytic equilibria existing in an IPG matrix can be described by the classical H–H equation:

$$\mathrm{pH} = \mathrm{p}K_i + \log \frac{[\mathrm{B}_i]}{[\mathrm{A}_i]} \tag{1}$$

where pK_i, as for any monofunctional weak acid or base, is a constant for each type of Immobiline, $[\mathrm{A}_i]$ is the molar concentration of the Immobiline in its acidic (protonated) form and $[\mathrm{B}_i]$ is the corresponding molarity of the Immobiline in its basic (non-protonated) form. The H–H equation and the electroneutrality conditions give the relation between the pH and the total concentration of Immobilines. If only two Immobilines are used, of which one can be regarded as fully ionized (titrant), the pH can be calculated directly from the Immobiline concentrations, with the aid of slightly modified H–H equations, depending on which species (an acid or a base) is used as a buffering group for an Immobiline gradient. If the buffer is an acidic Immobiline, it will be

$$\mathrm{pH} = \mathrm{p}K_\mathrm{A} + \log \left(\frac{C_\mathrm{B}}{C_\mathrm{A} - C_\mathrm{B}} \right) \tag{2}$$

whereas for a basic Immobiline, the corresponding expression is

$$\mathrm{pH} = \mathrm{p}K_B + \log\left(\frac{C_B - C_A}{C_A}\right) \quad (3)$$

where C_A is the molarity of the acidic Immobiline with $pK = pK_A$ and C_B is the molarity of the basic Immobiline with $pK = pK_B$. If the concentration of the buffering Immobiline is kept constant along the generated pH interval, the pH gradient resulting from linear gradient mixing will correspond to an ordinary titration curve. The best gradients with respect to linearity and buffering capacity, in such a case will be those having the mid-point centred on the pK value of the buffering species.

3.1.3. Narrow and ultra-narrow IPG gradients with mid-point centred or removed from the buffering pK

We have just seen (Fig. 7) that when a buffer is titrated in a pH interval from $pK + 0.5$ pH unit to $pK - 0.5$ pH unit a linear pH gradient will be generated by this titration process. We have plotted it in Fig. 8 (left): this is the simple case in which $| pH_m - pK | = 0$ (where pH_m = pH at the mid-point of our desired pH interval). In Fig. 8 we have also drawn the molarity of the buffering Immobiline (constant, zero slope), the molarity variation of the titrating (non-buffering) Immobiline (a line of negative slope, as we go from the acidic to the basic interval in titrating a basic buffer) and the profile of the accompanying buffering power (β): a dome-shaped, almost symmetrical curve with $\beta_{max} = pK$, just as expected. However, if we could work only under the condition $| pH_m - pK | = 0$, it would be a disaster, as only seven different pH gradients could be generated, centred on the pK of each of the seven Immobilines. Luckily, we can also work under the condition $| pH_m - pK | \neq 0$, by having the pH removed from the pK of the buffer by as much as ± 0.5 pH unit[4]: this gives us a practically unlimited number of pH intervals to work with. The results are shown in Fig. 8 (right). This time $pH_m = pK + 0.5$ pH unit, and yet we can still arrange for an almost linear pH gradient (solid curve) by generating also

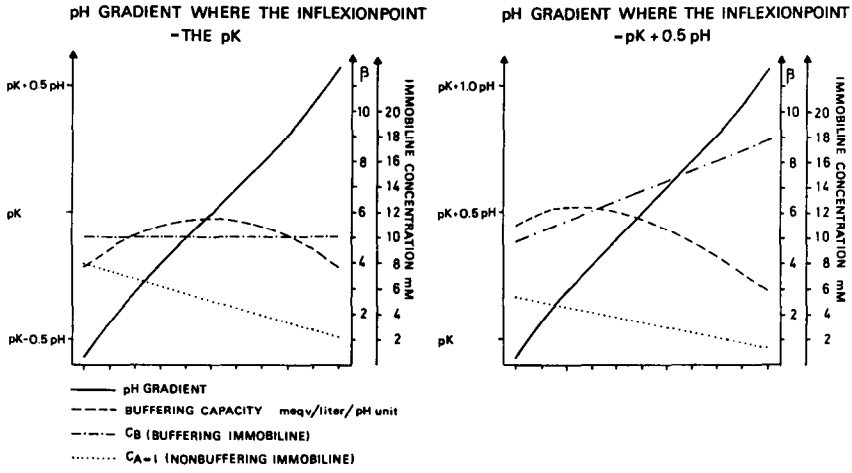

Fig. 8. pH gradients with midpoint (pH_m) centred or removed from the buffer pK. Left, $pH_m = pK$; right, $pH_m = pK + 0.5$ pH units. ———, pH gradients; , β power courses; · · · · ·, concentration course of titrants; · · · · , concentration courses of buffering Immobilines (courtesy of Dr. B. Bjellqvist).

a gradient of buffering species. As there would be much more buffering power at the acidic extreme (pH_{min}) of the pH interval (which, in this case, would be $pH_{min} = pK$), the concentration of the buffering Immobiline is progressively increased towards the basic extreme of our pH interval (line – · – · – of positive slope) so as to increase the β power in this region. The resulting β profile is now skewed, but it gives an acceptably linear pH gradient. The rationale for arriving at Fig. 8 (right) is as follows: from the H–H equation it is clear that a certain difference between a pH value and the pK defines a molar ratio between buffering and non-buffering Immobiline. If pH_m is the mid-point of the desired pH range, and if the concentrations of the acidic and basic Immobilines at pH_m are C_{A_m} and C_{B_m}, respectively, the pH, in distance relative to the mid-point, will be given by the expression

$$\Delta pH = pK - pH_m + \log\left[\frac{C_{B_m} + bx}{C_{A_m} - C_{B_m} + (a - b)x}\right] \tag{4}$$

if the buffering Immobiline is an acid, whereas if the buffering Immobiline is a base, the corresponding relation derived from eqn. 3 will hold. In this expression, x is the distance from the mid-point and a and b are dC_A/dx and dC_B/dx, respectively. From the criterion that $d^2pH/dx^2 = 0$, it is found that, in order to convert pH_m into the inflection point of the function $pH = f(x)$, the following relation should be satisfied:

$$a/b = \pm (2 - C_{A_m}/C_{B_m}) \tag{5}$$

where the negative sign results when the buffering Immobiline is a base. With the aid of this relation it is possible to generate any linear narrow pH range in the interval 3–10 with the aid of available Immobilines. As a general rule, in order to obtain a good buffering capacity with a minimum of incorporated Immobiline, the buffering species should have a pK value as close as possible to the pH of the mid-point of the pH gradient, while the non-buffering counter ion should have a pK so far away from the desired pH range that it can be regarded as fully ionized.

3.1.4. Selection criteria for 1 pH unit wide IPGs: the tandem principle

Table 2 gives a selection guide of some 1 pH unit pH intervals which can be generated with the aid of the presently available Immobilines. We work on a "tandem" principle, *i.e.*, knowing the desired pH interval, we select one Immobiline with the criterion that $pH_{min} < pK < pH_{max}$ (in other words, having the pK inside the limits of our pH interval; this is the general case, except in the intervals 4.9–5.9 and 7.3–8.3, where we have to work with "outside" pKs): this will be called the "buffering" Immobiline. We will then need a titrating Immobiline, which will be called "non-buffering", selected with the criterion that its pK will be as far away as possible from the desired pH interval (ideally pH_{min} or pH_{max} should be at least 3 pH units removed from the pK of the titrant). Under these conditions, the titrant Immobiline will be an "ideal titrant", *i.e.*, it will only provide equivalents of acid or base to titrate the buffering group but will not itself buffer in the desired pH interval. The guidelines on how to generate these pH gradients and on the calculations required are given below.

TABLE 2

SELECTION OF IMMOBILINES FOR 1 pH UNIT WIDE GRADIENTS

From LKB Application Note No. 321.

pH gradient desired (10°C, in gel)	*Immobiline*		*Buffering Immobiline*		*For ultra-narrow pH gradients within stated pH range, use nomogram No.*
	Buffering	*Non-buffering*	*An acid*	*A base*	
3.8– 4.8	p*K* 4.4	p*K* 9.3	+		I
4.0– 5.0	p*K* 4.6	p*K* 9.3	+		I
4.9– 5.9	p*K* 4.6	p*K* 6.2	+	+	III
5.7– 6.7	p*K* 6.2	p*K* 3.6		+	II
6.6– 7.6	p*K* 7.0	p*K* 3.6		+	II
7.3– 8.3	p*K* 7.0, 8.5	p*K* 3.6		+	–
8.0– 9.0	p*K* 8.5	p*K* 3.6		+	II
9.0–10.0	p*K* 9.3	p*K* 3.6		+	II

3.1.5. The use of nomograms

In practice, if we had to use each time eqns. 4 and 5 for deriving any desired narrow pH gradient, the calculations required would be laborious and might discourage the reader from ever entering the field. For your peace of mind, Dr. B. Bjellqvist has compiled three nomograms (whose use is suggested in Table 2), which can be found in the LKB Application Note 321 (August 1982), and which exemplify well the calculations needed. I report here nomogram I (to be used when the buffering Immobiline is an acid) in Fig. 9 and nomogram II (to be utilized when the buffering Immobiline is a base) in Fig. 10. Let us now take a practical example: suppose we want to focus human haemoglobins (Hb), Hb A, the adult species, has a p*I* (at 10°C) in IPGs of 7.3. We shall therefore prepare a 1 pH unit wide gradient, pH 6.8–7.8, so that Hb A will focus just in the middle of the pH gradient; the chances are that most Hb mutants will be found within this pH interval. The Immobiline with p*K* nearest to the mid-point (pH_m = 7.3) of the desired pH interval is the p*K* 7.06 species (at 10°C, in a 5% T gel; see Table 1). The nomogram to be used is thus No. II: it is entered on the far left column with the value of the difference $pK_B - pH_m = -0.24$ (see the arrow in Fig. 10). With the aid of a ruler set perpendicular to the vertical line of the far left column, and aligned on the −0.24 value, we draw a line that will intersect at right-angles columns 2, 3 and 4. At the intersection points, we read the following values: C_{B_m} = 10.9 m*M*, C_{A_m} = 3.95 m*M* and K_B = 3.4 m*M*. These values will be used to solve numerically the set of four equations at the bottom of Fig. 10, with the understanding that pH_a = 6.8 (this is the acidic extreme of our desired pH interval) and pH_b = 7.8 (this is the corresponding alkaline extreme). Thus:

$$C_{B_a} = 10.9 - 3.4\,(7.3 - 6.8) = 9.2 \text{ m}M;$$

$$C_{A_a} = 3.95\,[1 + 1.151\,(7.3 - 6.8)] = 6.2 \text{ m}M.$$

Symbols used in the nomograms and calculations

C = concentration of Immobiline in mol/litre

A, B = subscripts referring to acidic and basic Immobilines, resp.

$K_A = \frac{dC_A \text{ mol/litre}}{dpH \text{ pH unit}}$ $K_B = \frac{dC_B \text{ mol/litre}}{dpH \text{ pH unit}}$

Nomogram I (where the buffering Immobiline is an acid)

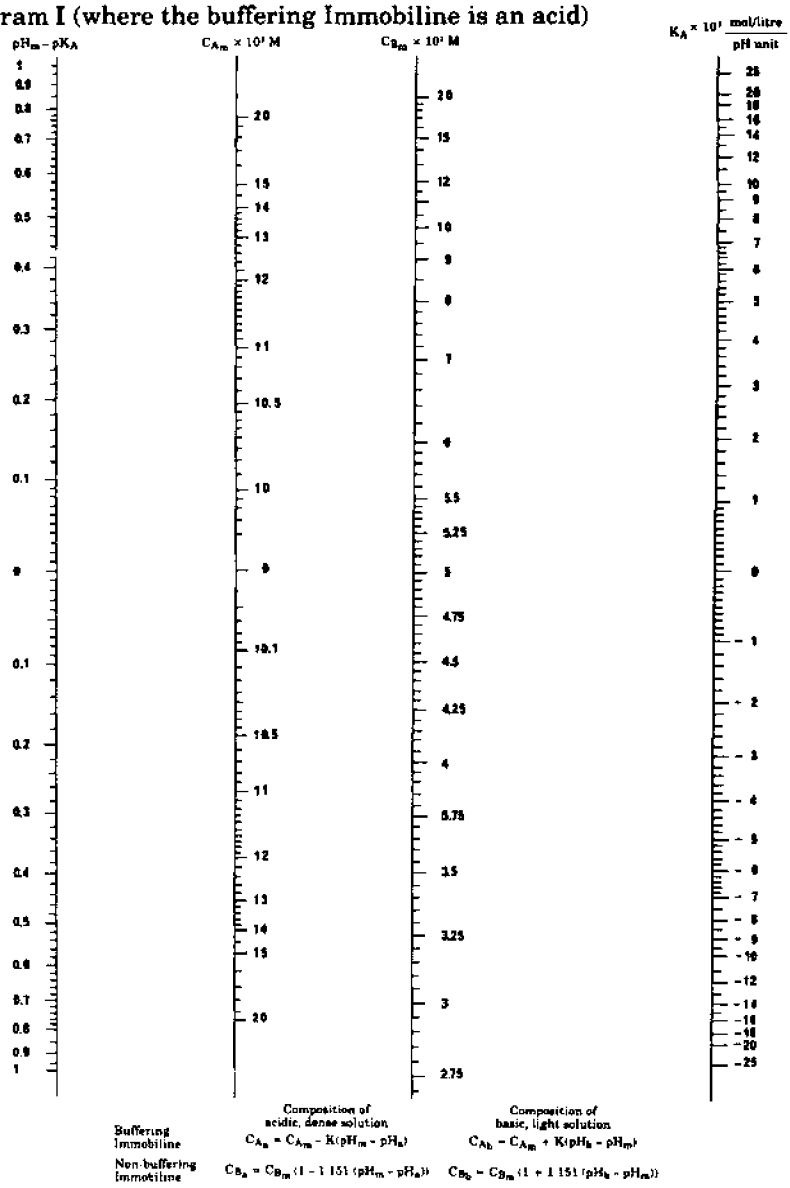

Fig. 9. Nomogram No. 1, to be used to calculate the amounts of buffering and titrating Immobilines in the dense and light solutions in the case in which the buffering species is an acid. For its use, see the example in the text (from LKB Application Note No. 321).

m = midpoint, subscript referring to the concentration, C, or pH at the midpoint of the pH gradient
a = subscript referring to the concentration, C, or pH of the acidic, dense solution used in gradient formation
b = subscript referring to the concentration, C, or pH of the basic, light solution used in gradient formation.

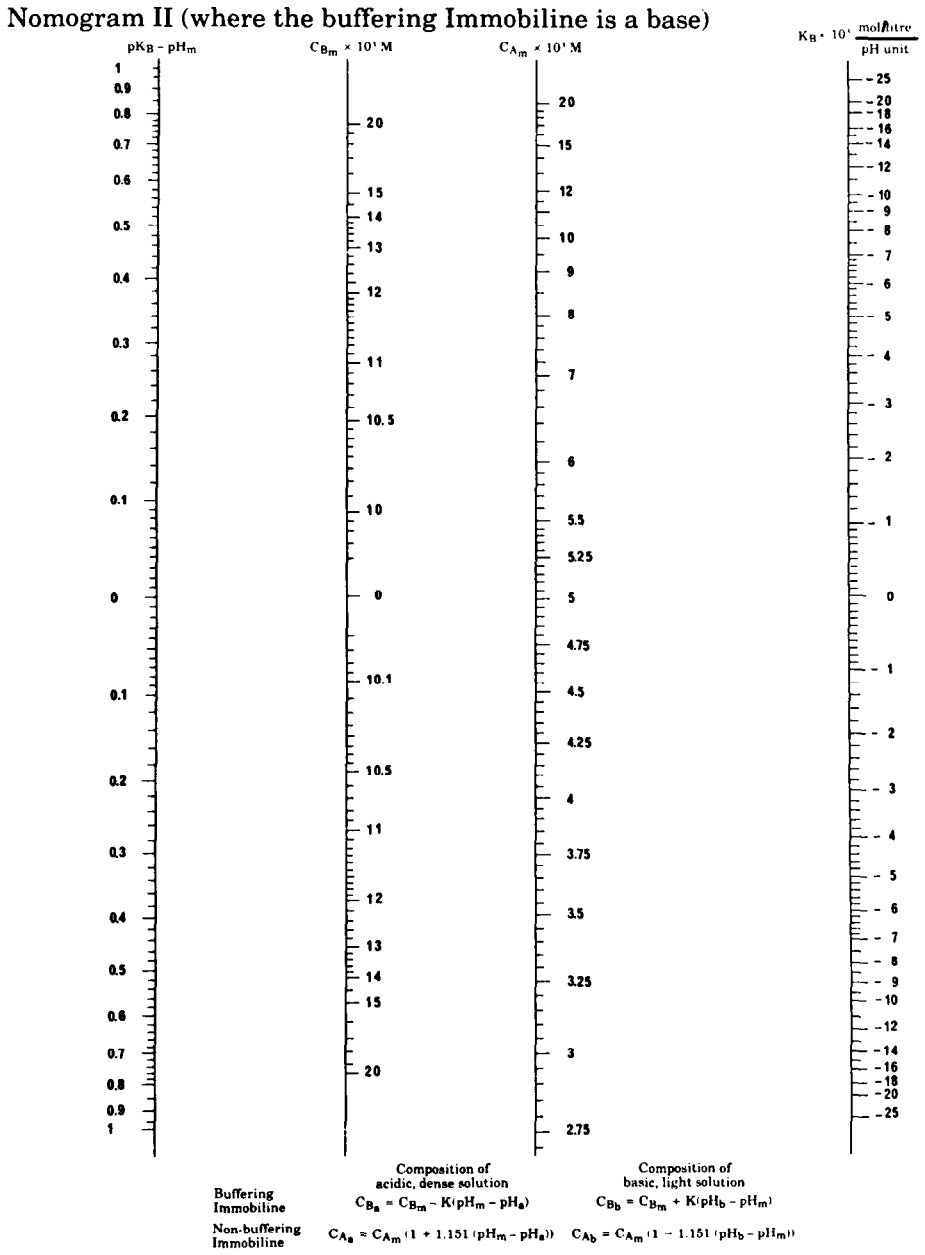

Fig. 10. Nomogram No. 2, to be used to calculate the amounts of buffering and titrating Immobilines in the dense and light solutions in the case in which the buffering species is a base. For its use, see the example in the text (from LKB Application Note No. 321).

Hence, if at the acidic extreme of our pH gradient we prepare a mixture of 9.2 mM Immobiline of pK 7.0 and 6.2 mM Immobiline of pK 3.6 (titrant) and we read its value at 10°C, it will give pH = 6.8. The second set of equations is needed for calculation of the composition of the basic, light solution. Accordingly:

$$C_{B_b} = 10.9 + 3.4\,(7.8 - 7.3) = 12.6 \text{ m}M;$$

$$C_{A_b} = 3.95\,[1 - 1.151\,(7.8 - 7.3)] = 1.68 \text{ m}M.$$

This means that, if the basic end of our pH gradient contains a mixture of 12.6 mM Immobiline of pK 7.0 and 1.68 mM of Immobiline of pK 3.6, the pH (at 10°C) will be 7.8. In practice, these nomograms are a combined, graphical representation of eqns. 4 and 5. By entering in nomogram II the value of the difference $pK - pH_m$ (see eqn. 4) we obtain directly the molarities of the buffering ion (C_{B_m}) and of the titrant (C_{A_m}) as calculated at the mid-point of the desired pH interval. However, as discussed above (Section 3.1.3), C_{B_m} cannot be kept constant as we would have too much buffering power at the acidic extreme (barely 0.2 pH unit removed from the pK of the buffer) and too little at the alkaline end (0.8 pH unit away from the pK 7.0 Immobiline). If $C_{pK\ 7.0}$ were kept constant, we would have a shallow pH gradient at the acidic end and a steep slope at the alkaline end. Thus, a correction factor is introduced which subtracts a given amount from the concentration of C_{B_m} to obtain C_{B_a} and adds back this same amount to C_{B_m} to generate the value of C_{B_b}; the rationale for this is to try to smooth the β power as much as possible over the desired pH interval. One last note: you will have noticed that the nomograms span a 2 pH unit interval, 1 above and 1 below the pK, and this is in contrast with what I have stated above (pK + 0.5 pH unit, see Section 3.1.1). In fact, this has been done for the sake of the calculations: I suggest you stay within the recommended interval (pK ± 0.5 pH unit), as outside these limits the scales are too compressed and the resulting errors very large; moreover, it will be very hard to compensate for the huge loss of buffering power at the "wrong" end of the pH interval.

3.1.6. Interpolation of ultra-narrow pH gradients based on the tandem principle

Let us go back to the above example, the separation of Hbs in a pH 6.8 7.8 gradient. We have just derived the molarities of the buffering and titrant Immobilines for the two extremes of our pH interval. In practice, for 125 × 110 × 1 mm gel dimensions, we shall mix in the acidic dense solution (the pH 6.8 extreme) 364 µl of 0.2 M Immobiline of pK 7.0 and 236 µl of 0.2 M Immobiline of pK 3.6 (for a total final volume of 8 ml) and for the basic chamber (the pH 7.8 extreme) the corresponding amounts will be 536 and 64 µl, respectively. Once the extremes of this pH interval have been calculated, any narrower pH range within the pH limits 6.8 and 7.8 can be derived by a simple linear interpolation of intermediate Immobiline molarities. Fig. 11 gives a graphical representation of the method employed: for instance, for resolving Hb San Diego from Hb A it was found necessary to operate over a narrow interval of 0.4 pH unit (pH 7.1–7.5). The limiting molarities of the two Immobilines in the 1 pH unit interval are joined by a straight line (because the pouring of the gradient from the two-chamber mixer is done linearly) and then the new pH interval

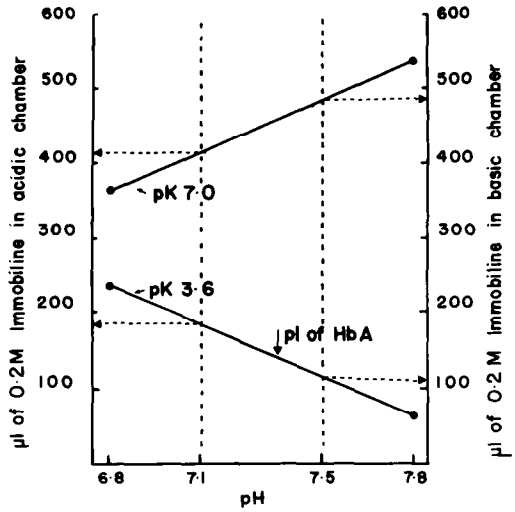

Fig. 11. Graphical representation of the preparation of narrow (up to 1 pH unit) IPG gradients on the "tandem" principle. The limiting molarities of p*K* 7.0 (buffering species) and p*K* 3.6 (titrant) Immobilines needed to generate a pH 6.8 7.8 interval are calculated with the aid of nomogram II in LKB Application Note No. 321 (see also Fig. 10). These points are joined by straight lines and the new molarities needed to generate any narrower pH gradient within the stated intervals are then obtained by simple linear interpolation (broken vertical and horizontal lines). In this example, a narrow pH 7.1 7.5 gradient is graphically derived (from Rochette *et al.*; see ref. 22).

is defined according to experimental needs (in our case, pH 7.1–7.5). Two lines are drawn from the two new limits of the pH interval, parallel to the ordinates (broken vertical lines). Where they intersect the two sloping lines defining the two Immobiline molarities, four new lines (broken with arrow heads) are drawn parallel to the abscissa and four new molarities of the two Immobilines defining the new pH interval are read directly on the ordinates. This process can be repeated for any desired pH interval, down to ranges as narrow as 0.1 pH unit. Within these limits (up to 1 pH unit) it is preferable to work on a "tandem" principle, *i.e.*, with only one buffering and one non-buffering Immobiline.

3.1.7. Casting of 2 pH unit wide gradients with multiple buffering species. Interpolation of narrow pH gradients

For Hb analysis and for screening of unknown samples, it might often be necessary to use a wide gradient, pH 6–8, as is customarily done in conventional IEF with carrier ampholytes[23]. The problem, which had not found an immediate solution when the IPG technique was first described[4], has now been solved with the aid of computer programs developed by Dossi *et al.*[24] and Gianazza *et al.*[25]. The data, for generating gradients 2 and 3 pH units wide, have been tabulated by Righetti *et al.*[26] and in LKB Application Note No. 322, and will be dealt with more extensively later (see Section 3.2.3). Fig. 12 shows graphically how to generate an Immobiline pH 6–8 gradient, with the aid of three buffering species (p*K* 6.2, 7.0 and 8.5) and one titrant (p*K* 3.6). The rationale in choosing the relative molarity ratios of the three buffers is again to try to keep the buffering power within the stated pH interval as constant as possible: this will automatically ensure minimum or no deviation from

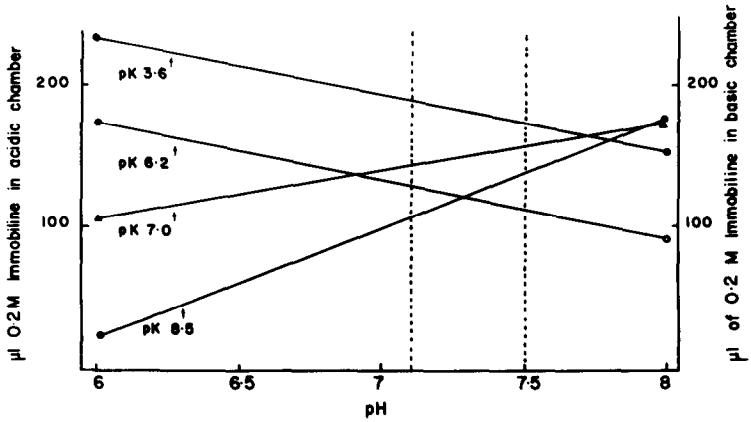

Fig. 12. Graphical representation of the preparation of wide (2 pH units) IPGs with multiple buffering species. The limiting molarities of the three buffers (p*K* 6.2, 7.0 and 8.5) and of the titrant (p*K* 3.6) needed to generate a pH 6 8 interval have been tabulated by Righetti *et al.* (see ref. 26 and Table 3 in this paper). By the same principle described in Fig. 11, once these points have been connected by straight lines, any narrower pH gradient within these limits can be derived by simple linear interpolation (the two vertical lines would represent the same, narrow pH 7.1 7.5 interval shown in Fig. 11). For clarity, the eight horizontal lines starting from the eight intercepts and going to the two ordinates, for calculating the new Immobiline molarities, have been omitted (from Rochette *et al.*; see ref. 22).

linearity of the generated pH gradient[25]. For 8 ml of solution in the acidic chamber (pH 6.0) the following volumes of buffers have been used: 235 µl of p*K* 3.6, 177 µl of p*K* 6.2, 108 µl of p*K* 7.0 and 24 µl of p*K* 8.5 Immobilines; for the corresponding 8 ml of solution at the other extreme (pH 8.0), the volumes were 156 µl of p*K* 3.6, 96 µl of p*K* 6.2, 17 µl of p*K* 7.0 and 180 µl of p*K* 8.5 Immobilines. Again, by a linear interpolation of these limiting molarities, any narrower pH gradient within these two extremes can be derived graphically. In Fig. 12 the computation of the same narrower pH 7.1–7.5 gradient described above is shown (broken vertical lines). Experiments performed in these two different types of narrow pH gradients have given identical results[22], although it is much simpler, below a 1 pH unit interval, to work with the "tandem" approach.

At this point, having seen so many calculations and simulations but no real separations, you might want to quit in despair. Perhaps Fig. 13 will change your mind: there is nothing exceptional in this separation, done in a 0.8 pH unit interval (pH 6.9–7.7; the narrower pH 7.1–7.5 gradient mentioned above was used for preparative runs); as we can work in only a 0.1 pH unit span, we can pull the two bands further apart by a factor of eight. What is striking is that, when Hb San Diego was first described in 1974, Nute *et al.*[27] reported that this mutant could not be separated from HbA by any known chromatographic or electrophoretic technique (including conventional IEF). Hb San Diego is a typical "electrophoretically silent" mutant (a valine to methionine substitution): may I suggest that with the presently available IPG technique nothing is silent any longer? Another example of a very difficult separation problem is the resolution between Hb S and Hb D, which essentially co-focus in the same zone. By "engineering" a pH gradient centred on the p*I* of Hb S, we

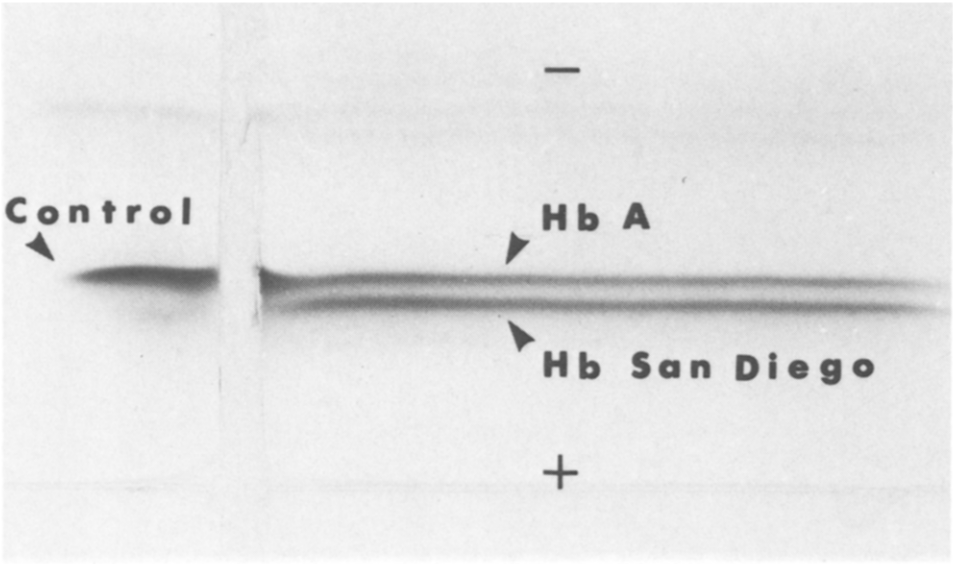

Fig. 13. Separation of Hb A from Hb San Diego by IPG. The analytical gel was 125 × 110 mm, 1 mm thick and contained 5% T and Immobilines of pK 7.0 and pK 3.6 in such ratios as to generate a 0.8 pH unit span (see Fig. 11) from pH 6.9 to 7.7. About 8 mg of total protein were loaded in the right trench. In the left pocket, 1.5 mg of Hb from a normal adult lysate was applied. The ΔpI between Hb A and Hb San Diego was estimated to be 0.01 pH unit (from Rochette *et al.*; see ref. 22).

could amply resolve the two species over a 0.4 pH unit span (pH 7.4–7.8) without even having to push the IPG technique to its limit (taken at present as a separation over a 0.1 pH unit range) (see Fig. 14). Both pH ranges utilized in Figs. 13 and 14 were calculated either from Fig. 11 or from Fig. 12, with identical results although, obviously, for ultra-narrow pH gradients, it does not pay to have to resort to the use of multiple buffering species.

3.1.8. Resolving power

As derived by Rilbe[28], the resolving power in IEF is given by

$$\Delta \mathrm{p}I = 3 \sqrt{\frac{[D\ \mathrm{d(pH)/d}x]}{[E - \mathrm{d}u/\mathrm{d(pH)}]}} \tag{6}$$

where D = diffusion coefficient of a protein having a titration curve (pH/mobility slope) of du/d(pH), E = electric field strength (V/cm), d(pH)/dx = slope of the pH gradient in the IEF gel and ΔpI = difference in isoelectric points between a protein and the nearest resolvable contaminant. In order to increase the resolving power, we have to find experimental conditions that minimise the value of ΔpI. There are three ways in which this can be done: (a) decrease the numerator; (b) increase the denominator; (c) simultaneously increase and decrease both. However, some parameters in

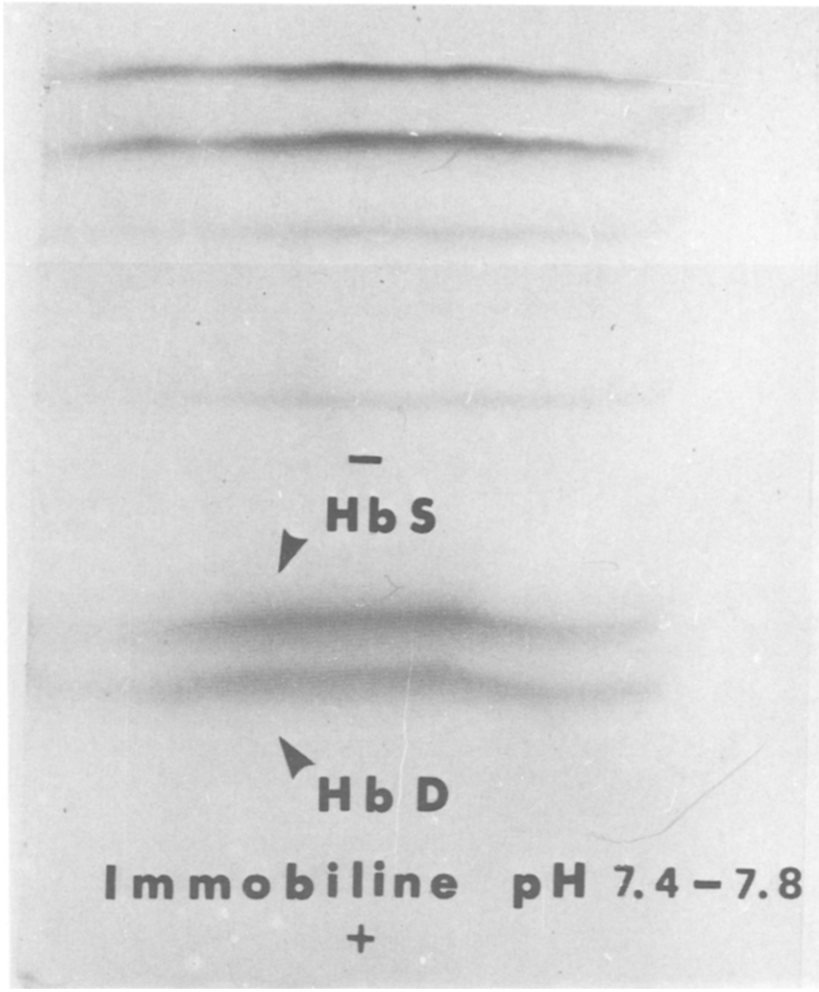

Fig. 14. Separation of Hb S from Hb D by IPG. All conditions as in Fig. 13, except that the run was in an IPG gradient of pH 7.4 7.8. The run was carried out overnight at 2000 V and 10°C. The sample (8 mg total mixture) was applied in a trench at the anode. The ΔpI between Hb S and Hb D was estimated to be 0.005 pH unit (from Gelfi and Righetti, unpublished work).

this equation cannot be manipulated: for any given protein, D is constant and proportional to mass and $du/d(pH)$ is constant and proportional to charge, and that is the end of it. Here is where the "magic" of Immobiline pH gradients step in: as the conductivity is extremely low (*ca.* one hundredth of the value for CA gels) and as the pH gradient width can be mathematically determined, we can *simultaneously decrease d(pH)/dx and increase E almost at leisure*. The resulting resolving power is almost unbelievable: $\Delta pI = 0.002$ in a 0.01 pH unit/cm gradient[16]. This can be appreciated in Fig. 15: when a commercial ovalbumin sample was run in a conventional Ampholine pH 4–6 gradient, with a slope of *ca.* 0.2 pH/cm, it was resolved

into a number of bands, of which the dark, central band (A) appeared as a single, homogeneous component. However, when the same sample was run in Immobiline gels of only 0.02 pH/cm (C, 0.2 pH unit interval across the entire gel length), this major band was clearly split into two components[4]. The p*I* difference between these two bands was estimated to be 0.002 pH unit, which corresponds to a charge difference between the two species of only 2/100 of a unit proton charge (probably these two bands represent the same protein existing in equilibrium between two different conformational sub-states). This is a far cry from the resolution limit for conventional IEF given by Vesterberg and Svensson[29] as a $\Delta pI = 0.02$ pH unit. If we compare IPGs with the leading electrophoretic technique of the 1960s, disc electrophoresis[30], the increment in resolution is even more striking: in the latter technique, two species would be resolved only when the difference in surface charge was of the order of 1 proton unit.

3.2. Extended pH gradients

We have seen, so far, the generation of narrow and ultra-narrow IPGs; there are cases, however, when it might be advantageous to mix two or more buffering Immobilines, in order to cover wider pH intervals, to be used as the first dimension of two-dimensional (2-D) techniques. 2-D maps are most sensitive to disturbances in the first dimension (*e.g.*, cathodic drift, near isoelectric precipitation) which lead to altered or blurred spots in the final 2-D plane. The insensitivity of grafted pH gradients to such disturbances, and the ease of control of the form and width of these gradients make them the natural choice for this application. There appear to be three

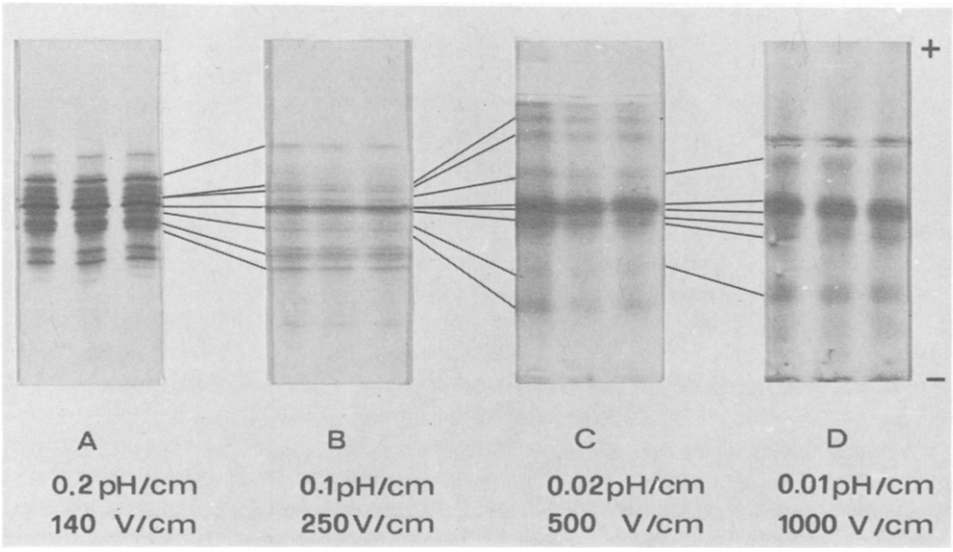

Fig. 15. Ovalbumin focused on a narrow Ampholine pH gradient (A) and on Immobiline gradients with varying pH slopes (B D). Strips B D contain 5×10^{-3} *M* Immobiline of p*K* 4.6 titrated with Immobiline of p*K* 9.3 to the respective pH slopes. Ovalbumin loads in the sample tracks (from left to right): 40, 20 and 20 μg (from Bjellqvist *et al.*; see ref. 4).

ways of producing wide pH gradients (>2 pH units) with Immobilines: (a) multi-chamber mixers; (b) two-chamber mixers with identical molarities of buffering species and varying concentrations of titrants; (c) two-chamber mixers containing different amounts of the same Immobiline species. I shall review here these three approaches, hoping not to end up in total confusion.

3.2.1. Multi-chamber mixers

It was in the summer of 1982 that Giulio, Fabrizio, Elisabetta and myself started out to solve the problem of generating wide pH gradients. The collaboration was hectic at times. At one point, Fabrizio disappeared in a sailing expedition in the Mediterranean and we could not reach him even by satellite. We had to drive down to Ancona, on the Adriatic seashore, and send messages in bottles to re-establish communications. We started out with a pestiferous gadget, a nine-chambered mixing device designed by Peterson and Sober in 1959[31] and adapted to the Technicon Analyzer for amino acid elution. If the nine chambers are filled equally with nine

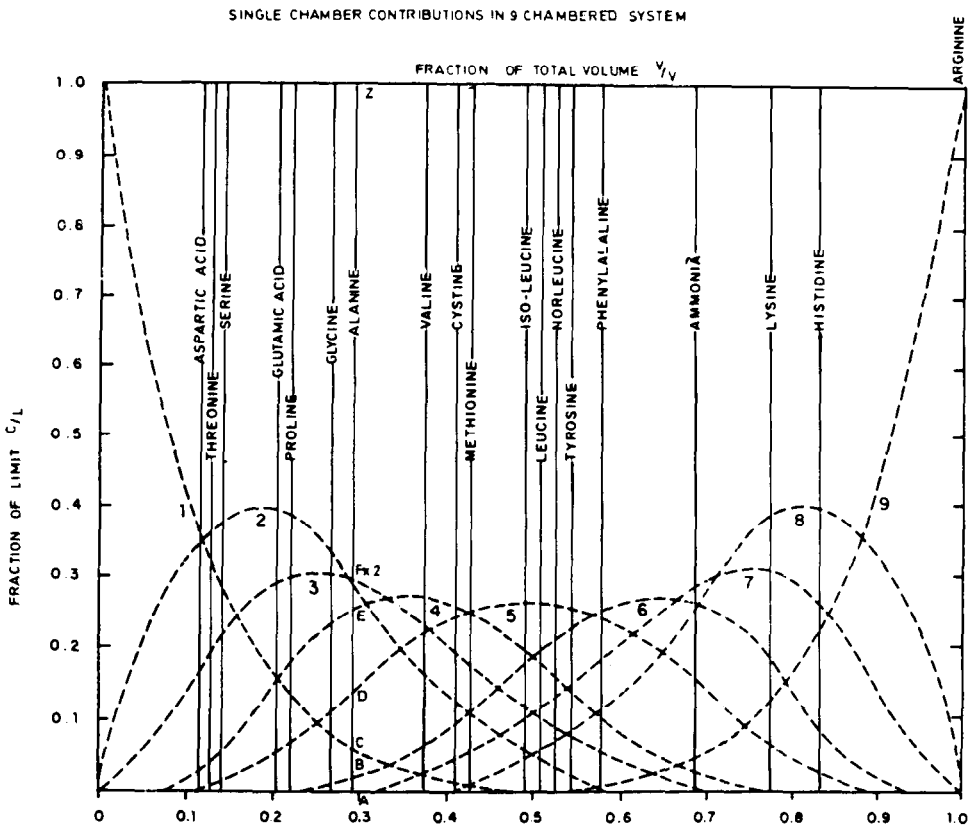

Fig. 16. Composition of the eluate from a nine-chambered gradient in terms of the contribution of each buffer in a single chamber (numbered 1-9). The vertical lines represent the elution position of each amino acid from the Autoanalyzer when using a Varigrad for mixing the eluent buffers (modified from Peterson and Sober; see ref. 31).

different solutions, it can be demonstrated that the elution profile will be as depicted in Fig. 16: only the solutions in the first and last chambers will exhibit an exponential decay, reaching zero concentration in the middle (chamber 5) and only the solution in vessel 5 will show a symmetrical distribution (a dumbbell-shaped function). In all other chambers the elution profile will be skewed, with the distribution curves of chambers 6, 7 and 8 being the specular image of vessels 4, 3 and 2, respectively. An important lesson was learned from this graph: if we were to place in each chamber a different Immobiline, in order of increasing pK, titrated to increasing pH values, by elution under appropriate conditions we could not only generate a linear pH gradient, but could also confine each Immobiline species to the pH interval in which it would exhibit maximum buffering power. On a hot and humid day in July, Giulio appeared in our laboratory with the gadget shown in Fig. 17: a five-chambered mixer in which five of the seven available Immobilines were used as buffers (a single species in each chamber) and the remaining two as titrants (the pK 3.6 acid for the three bases and the pK 9.3 base for the two acids)[24]. We made at least one basic mistake, though: we used two acids (pK 4.4 and 4.6), with adjacent pKs, in the same mixture, so that we could never straighten up the acidic end of our pH gradient (too much buffering power —remember what we stated in Section 3.1.5). For that matter, we could never maintain a linear course also at the alkaline extreme, and that was the

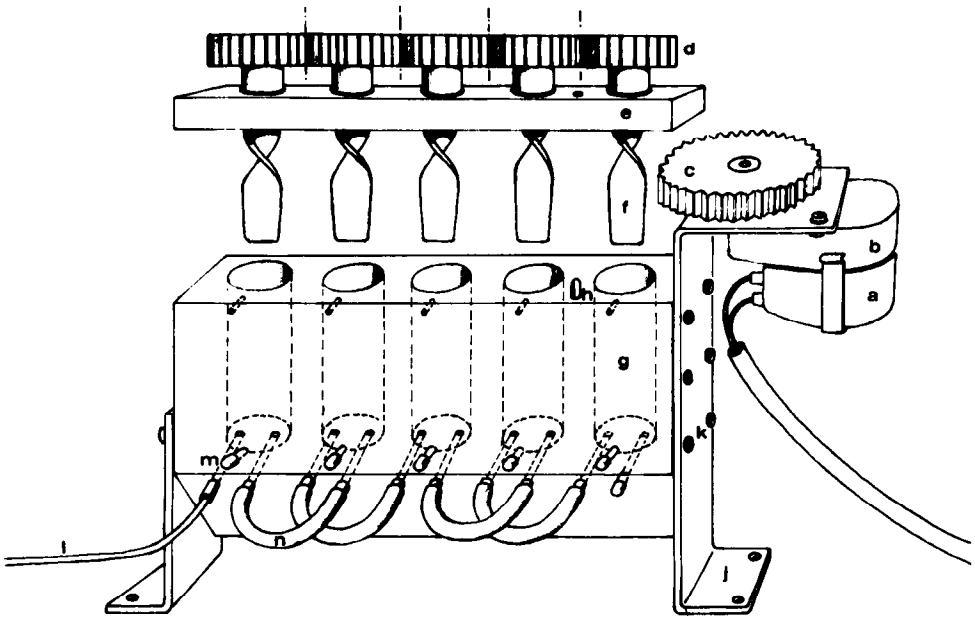

Fig. 17. View of the five-chamber gradient mixer of Dossi *et al.* (see ref. 24) (the stirring pad block is lifted). Letterings: (a) motor (power = 3 W, 24 V a.c.); (b) reduction unit (60 rpm); (c) driving gear (nylon, 80 mm diameter, 80 teeth); (d) transmitting gears (30 mm diameter, 30 teeth); (e) ball-bearings housing (rigid double crown; O.D. = 22 mm, I.D. = 15 mm; h = 7 mm); (f) stirring paddles (Plexiglass spiral, 70 mm long, 20 mm top and 12 mm bottom width, fitted in the hub of a cylindrical block); (g) Plexiglass block with five cylindrical chambers; (h) pins for fastening the stirring paddle unit to the multi-chamber block; (i) air vents; (j) supporting feet; (k) screws for assembling the feet to the block; (l) outlet to the pump; (m) drain tubes; (n) connecting tubes.

second mistake, to try to titrate the upper end to a pH outside the last available pK. In connection with this, a computer program was developed which, given the molarity and type of Immobiline in each chamber, would predict the course of the pH gradient generated, together with the buffering capacity (β) and ionic strength (I) profiles associated with that particular pH range. For that, we had to derive some basic equations describing the system. By writing the equilibrium constants of the dissociation of acidic and basic Immobilines, and considering the electroneutrality law, we can derive the first one:

$$\sum_{j=1}^{l} [B_j^+] \frac{[H^+]}{[H^+] + K_j} - \sum_{i=1}^{m} [A_i^-] \frac{K_i}{[H^+] + K_i} = 0 \tag{7}$$

where $[A_i^-]$ and $[B_j^-]$ are the molar dissociated fractions of acidic and basic Immobilines, respectively, and K_i and K_j are the numerical values of their respective pKs. Eqn. 7 is a polynomial of degree $m + 1$ in $[H^+]$. This equation can be solved numerically by Newton's approximation when the actual concentrations of all the Immobilines in the output flow are known. These can be calculated with the generalized Peterson–Sober equation[31]:

$$C_i = \sum_{j=1}^{N} L_{ij} \frac{(N-1)!}{(N-j)!(j-1)!} \left(1 - \frac{v}{V}\right)^{N-j} \left(\frac{v}{V}\right)^{j-1} \tag{8}$$

where C_i is the output concentration of species i, L_{ij} is the initial concentration of species i in the jth chamber, N is the number of chambers used, V is the total volume in the system and v is the dispensed volume.

This approach was clever in a way, but required laborious manipulations and too much care in handling the solutions, so we realized it was bound to end up in a dusty corner in a science museum (much to my surprise, however, on a recent visit to the Zurich Polytechnic I found a second apparatus built by Dr. Lutz, so there are now two museum pieces in the world). We were thus forced to resort to a second approach, outlined below.

3.2.2. Two-chamber mixers with identical buffer concentration

The problem of generating extended pH gradients with a two-chamber mixer could have two different solutions. In one approach, a two-chamber device of non-identical cross-section is used. The mixture of buffering components, titrated with a non-buffering species to one extreme of the pH interval, is placed in the mixing chamber, while the titrant, needed to bring the mixture to the other extreme of the chosen pH range, is filled into a reservoir of highly reduced cross-section. In this system, however, because the volume in the reservoir is small in comparison with the volume of the titrated solution, and assuming that the pK of the titrant is well outside the generated pH interval, so that it is fully dissociated throughout, an exponential pH gradient is generated whose slope depends on the ratio of the two volumes.

In another approach (the one finally adopted), a mixer having two chambers of identical cross-section is used. In this case, the eluate contains linearly increasing amounts (from 0 to 100%) of the species present in the reservoir and linearly decreasing amounts (from 100 to 0%) of the compounds initially present in the mixing chamber. This behaviour, fully predicted by eqn. 8, suggests the use of the same buffering species, in identical concentrations, in both chambers of the gradient mixer, titrated with the aid of non-buffering Immobilines (fully dissociated in the entire interval of the generated pH gradient) to the two extremes of the desired pH interval. During the elution, the concentration of the buffering species is strictly constant while the concentration of the non-buffering compounds in the eluate varies linearly, thus giving a true titration of the buffering groups. The buffering power (β) is defined as

$$\beta = dB/d(pH)$$

where dB and d(pH) are infinitesimal variations of the titrated species and of pH, respectively. Eqn. 8 shows that the titrant concentration changes linearly as a function of the eluted volume (v); therefore

$$dB/dv = \text{constant} \tag{10}$$

Therefore, as under our experimental conditions we aim at generating linear pH gradients, which is to say

$$d(pH)/dv = \text{constant} \tag{11}$$

it follows that, by substituting eqns. 10 and 11 into eqn. 9,

$$\beta = \text{constant} \tag{12}$$

In other words, *the fundamental requirement for generating a linear pH gradient is that the buffering power is constant throughout.* For optimization of the pH gradient linearity, the most convenient solution is to keep varying the relative concentrations of the buffering species, until the β power reaches a constant value in the desired pH interval. For this purpose, in the computer program described above, we have introduced a procedure for optimizing the composition of the solutions used in the mixing chambers. This algorithm minimizes the coefficient of variation of the buffering capacity (β), in the interval of the generated pH gradient, by progressively varying the relative concentrations of the buffering species until peaks and valleys of β power are flattened out[25]. A comparison between the multi-chamber and two-chamber mixer approaches is shown in Fig. 18. In both instances a fairly linear pH 4–9 gradient is generated, with a reasonably smooth β power and an acceptable ionic strength profile (the two-chamber approach appears better because the Immobiline mixture could be optimized with the aid of the improved computer program). The solution adopted for generating a 5 pH unit interval with the two-chamber device is by far the simplest: a single mixture of buffering species (pK 3.6, 4.6, 6.2, 7.0, 8.5 and 9.3) is made, with relative molarities optimized in terms of constant β power and pH gradient linearity (for its composition see Table 5 in ref. 25). This solution is then divided into two equal portions: to one enough equivalents of pK < 1 Immobiline are added to lower

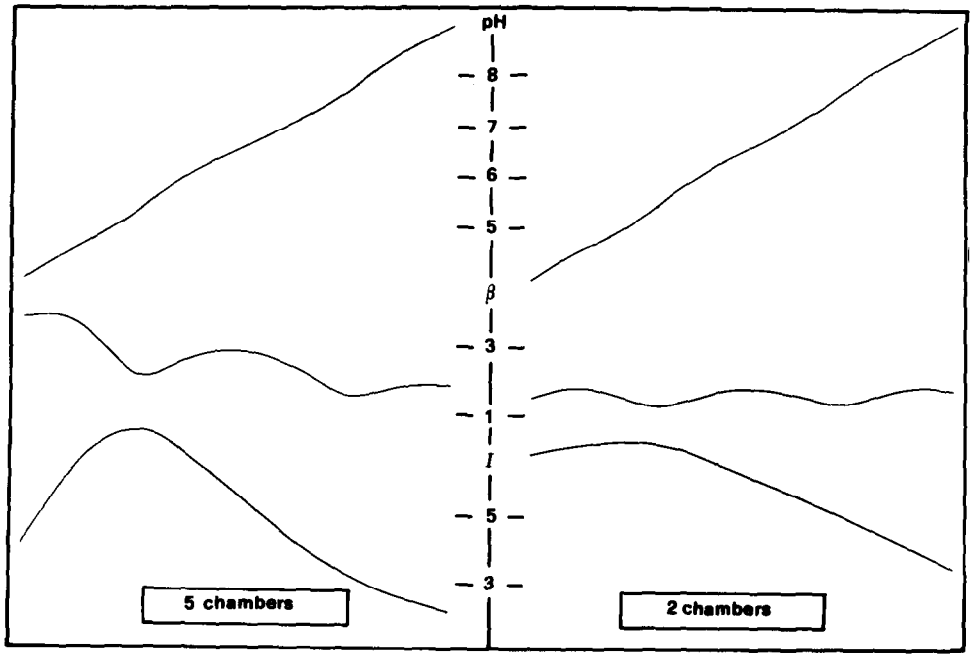

Fig. 18. Generation of extended IPG intervals. A 5 pH units gradient (pH 4–9) was generated with either a five- or a two-chamber mixing unit. In both instances the accompanying buffering powers (β) and ionic strengths (I) are plotted (from Righetti *et al.*; see ref. 16).

the pH to 4 (or any other desired value); the other is titrated with the proper amount of pK 9.95 Immobiline required to reach the other extreme of the pH interval (pH 9, or any other desired pH span). However, the multi-chamber approach was valuable to us for at least one practical reason: in the absence of commercially available titrant Immobilines (*i.e.*, species with pKs well outside the desired pH span), only this device allowed the generation of the same pH 4–9 interval with the use of buffering species alone, thus disposing of non-buffering titrants.

3.2.3. Two-chamber mixers with different buffer concentrations

The third approach, suggested by Dr. B. Bjellqvist, was still to use a two-chamber mixer, but with varying concentrations of the buffering species in the two vessels. At present, 14 pH intervals have been pre-calculated, as shown in Fig. 19: one of 1.5 pH units (pH 3.5–5), nine spanning 2 pH unit intervals, in 0.5 pH unit increments (e.g., pH 4–6, pH 4.5–6.5; pH 5–7 and so on, up to pH 8–10) and four encompassing 3 pH units, in 1 pH unit increments (from pH 4–7 up to pH 7–10). The recipes for each interval are given in Table 3: it can be seen that they are all based on the principle of multi-buffering species (see also Section 3.1.7). As stated previously (see Sections 3.1.6 and 3.1.7) the limiting molarities in each chamber can be plotted on a graph, connected by a straight line, and then each narrower pH gradient within the stated limits can be interpolated as shown in Figs. 11 and 12. These recipes have been calculated so as to give an average buffering capacity in the gels of about 3 mequiv. l^{-1} (pH unit)$^{-1}$, a value which will be adequate for most ap-

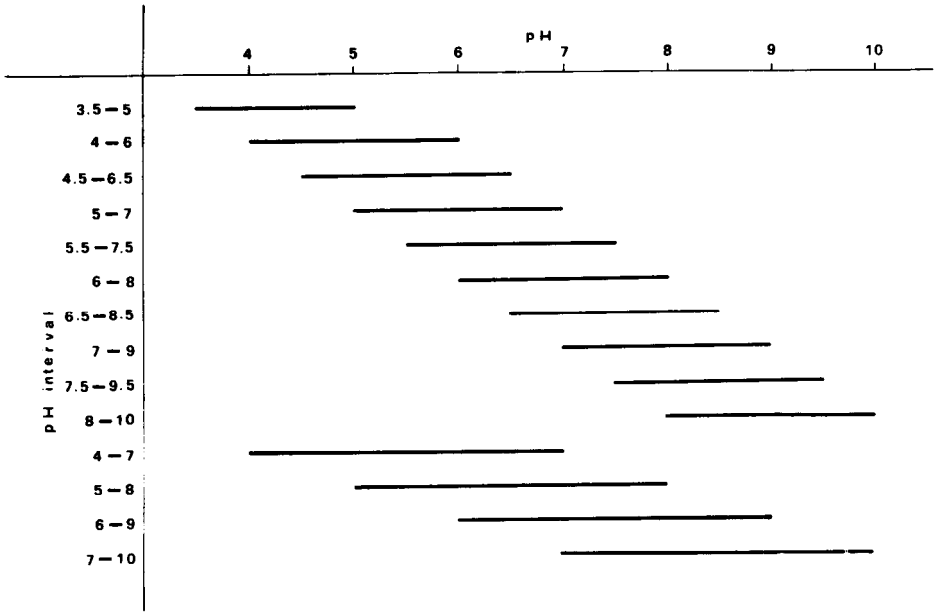

Fig. 19. Pre-calculated pH intervals at present available: one of 1.5 pH units, nine of 2 pH units and four of 3 pH units. For the recipes giving the limiting compositions in the two chambers see Table 3 (from LKB Application Note No. 322).

TABLE 3

PREPARATION OF 2 AND 3 pH UNIT INTERVALS

From Righetti *et al.*; see ref. 26.

pH range (10°C)	*0.2 M Immobiline (μl)*											
	For 15 ml of acidic solution						*For 15 ml of basic solution*					
	pK 3.6	*pK 4.6*	*pK 6.2*	*pK 7.0*	*pK 8.5*	*pK 9.3*	*pK 3.6*	*pK 4.6*	*pK 6.2*	*pK 7.0*	*pK 8.5*	*pK 9.3*
3.5–5	394	285	161	–	–	–	263	398	589	–	–	–
4 –6	619	107	473	–	–	–	422	563	299	–	–	782
4.5–6.5	450	261	540	–	–	–	–	615	263	255	–	323
5 –7	69	431	414	–	–	–	–	483	276	224	–	328
5.5–7.5	–	440	347	111	–	–	340	–	232	281	278	–
6 –8	441	–	333	203	45	–	293	–	178	333	338	–
6.5–8.5	824	–	294	194	576	–	205	–	164	302	387	–
7 –9	1378	–	–	277	380	863	491	–	–	236	194	557
7.5–9.5	722	–	–	480	244	375	221	–	–	998	150	375
8 –10	350	–	–	325	308	84	81	–	–	293	325	254
4 –7	619	107	473	–	–	–	323	791	161	287	–	940
5 –8	799	285	469	150	394	–	199	141	150	394	394	–
6 –9	728	–	375	86	338	75	225	–	150	420	225	210
7 –10	558	–	–	389	361	–	92	–	–	333	361	289

plications. I have to point out that these recipes will only give the pH gradients stated in the left column when the IEF run is performed at 10°C (the reason is to be found in Table 1 and Fig. 3). The amounts of Immobiline stated in Table 3 refer to a total final volume in each chamber of 15 ml, enough for preparing two gels 0.5 mm thick. There is still some information missing: three pH gradients of four pH units, two spanning five pH units and one covering the broad pH 3.5–9.5 interval. We are only a few computation days away from these results, after which running Immobiline gels will be just as easy as reading a recipe from a cook-book (I hope, though, you are still able to distinguish the flavours of Italian and Swedish cooking; if not, you will have no problems in settling in Sweden).

3.2.4. Computer simulations

The computer program we have developed (Dossi and Celentano, Copyright 1982) has helped us to understand to a greater depth the basic behaviour of immobilized pH gradients; in fact, such a sophisticated technique would be misused if one could not control the experimental parameters and the possible sources of errors connected with the dispensing of the Immobiline chemicals. I should also like to add that this knowledge is not just strictly related to IPGs: the basic principles will also apply to separations in ion-exchange chromatography and chromatofocusing, thus greatly broadening our horizons. Here are some examples of the applications: greater details were given by Gianazza *et al.*[25].

3.2.5. How to smooth the β power (see also Section 3.5)

As a constant β power appears to be fundamental for generating linear pH gradients with the above approaches, we have simulated the behaviour of the β course as a function of the ΔpKs of the buffers. As shown in Fig. 20, the smoothest power course is obtained when buffers have evenly spaced pKs at 1 pH unit intervals. As the ΔpKs are increased, peaks and valleys and β power become more pronounced, with concomitant increments of pH deviation from linearity. Conversely, nothing is gained if ΔpKs are progressively decreased below 1 pH unit, as already at $\Delta pK = 1$ a very linear pH gradient (deviation ± 0.003 pH unit) and a fairly smooth β power are obtained. What is detrimental to pH gradient linearity, therefore, is an uneven distribution of the pKs of the buffers. One practical consequence is immediately apparent: when generating extended pH gradients, Immobilines of pK 4.4 and 4.6 should never be mixed together. This is a far cry from conventional pH gradients with carrier ampholytes, where it had been calculated that a minimum of 20 species, evenly spaced at $\Delta pI = 0.05$, were required per pH unit for generating a stepless pH course[23] (in reality, there might be a few hundred species per pH unit). We have learned another interesting lesson from our computer simulation: when presently available Immobilines are titrated over 4 pH units (pH 4.5–8.5), a fairly even β power throughout can be arranged, which is still fairly well maintained when this range is extended to 5 pH units (pH 4–9). However, as soon as the pH interval is extended to pHs outside pK_{min} and pK_{max} of the components of the mixture (*e.g.*, pH 3.5–9.5), two sharp hills of β form at the two extremes, and the pH gradient loses its linear course.

What is an acceptable deviation from linearity in our IPG system? We have taken as a maximum deviation 1% of the stated pH interval (in pH units). Thus, in

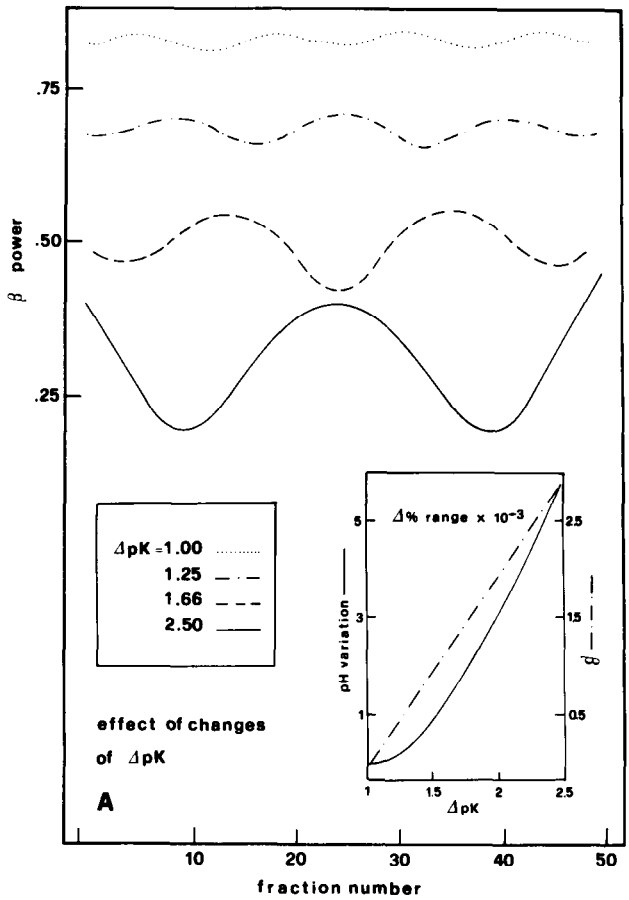

Fig. 20. Effect of changes in the number of (evenly spaced) buffering components. The optimal concentrations of fictitious buffers (bases), with p*K*s differing by 1, 1.25, 1.66 and 2.5 pH units, were calculated so as to cover the pH range 4.5–8.5. The resulting courses of β power are shown as a function of ΔpK. The inset is a plot of the percentage variation, in comparison with the case $\Delta pK = 1$, of the ranges of deviation of pH (left-hand scale) and of β (right-hand scale) (from Gianazza *et al.*; see ref. 25).

a 1 pH unit interval, the maximum acceptable deviation will be 0.01 pH unit, and so on. In practice, it is possible to do better than that: in the pH ranges tabulated in Table 3, the deviation from linearity is of the order of a few thousandths of a pH unit.

3.2.6. How to choose the titrants

The need to have strongly acidic and strongly basic titrants, for generating wide pH intervals, was immediately apparent from Fig. 20. I have previously defined a titrant as a species that is fully dissociated in the desired pH interval: if it becomes progressively undissociated it means that it has a p*K* within the operative pH range and as such it will behave as a buffer and will automatically influence the pH course. In Fig. 21 we have simulated the case of an acidic titrant: as long as the distance between pH_{min} and the titrant p*K* is above 2 pH units, this compound will behave as

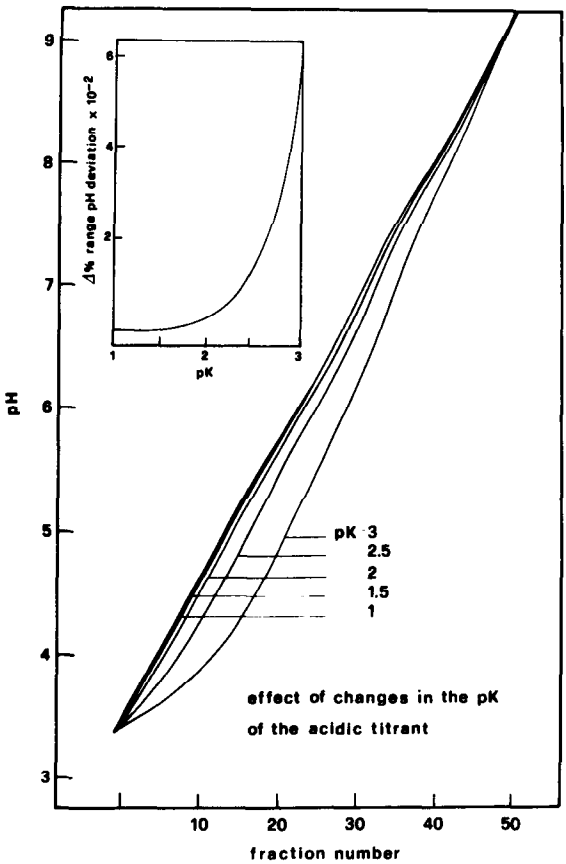

Fig. 21. Effect of changes in the pK of the acidic titrant. A reference Immobiline mixture was titrated to the same pH value with fictitious acids whose pK was 0.5, 1.0, 1.5, 2.0 and 2.5 pH units lower than the gradient's limit (in this case, pH_{min} = 3.5), and the pH course was calculated for the five cases. The inset is a plot of the percentage variation of deviation of pH from linearity as the titrant's pK increases (from Gianazza *et al.*; see ref. 25).

an ideal titrant and will not affect the slope of the desired pH gradient. However, as pK − pH_{min} becomes smaller than 1, the acidic portion of the pH curve will be flattened out; when this distance is only 0.5 pH unit, the effect on the pH gradient will be felt even up to alkaline pH (pH 8 and above) (see Fig. 21). The same reasoning will apply to the alkaline branch of the pH gradient in the case of a basic titrant.

3.3. How to deal with experimental errors

If we believe in the properties of Immobilines and in the H–H equation (eqn. 1), there should be no doubt that highly reproducible pH gradients should be obtained run after run. However, as we do not live in an error-free environment, the reproducibility of our system will be only as good as our ability to minimize experimental errors. The most dramatic effect will be given by inaccuracy in dispensing the Immobiline chemicals, as their concentration ratios determine the width and slope

of the wanted pH gradient and as, in thin gels, the volumes required are small, usually of the order of a few microlitres. Fig. 22 shows a plot of the deviation of the expected pH gradient as a function of an inaccuracy of measurement of 2%, for an acidic buffering species (broken line) and for a basic Immobiline (solid line). The ordinate represents the deviation from the desired pH interval (pH expected − pH observed), plotted as a function of the distance between the prevailing pH in solution and the pK of the buffering ion (pH − pK) on the abscissa. The two curves are reciprocal, symmetrical exponentials with a cross-over point at pH − pK = 0 (the point of maximum buffering power, remember!). With an acidic buffering Immobiline, at negative pH − pK values the error becomes progressively negligible, being only 0.01 pH unit when the pH in solution is 1 unit below the pK (at this pH value the carboxyl group will be 90% protonated); however, on the opposite side, when the solution pH is 1 unit above the pK (and therefore the acid is 90% dissociated) the effect of a 2% inaccuracy becomes more relevant, giving a deviation 10 times higher than in the former case (0.1 pH unit). The same reasoning, but with a "mirror image", applies when the buffering Immobiline is a base: the minimum pH deviation (0.01 pH unit) will be expected at a pH 1 unit above the pK (where the base is 90% deprotonated) while the maximum deviation (0.1 pH unit) will be found at a pH 1 unit below the pK (where the base is 90% protonated).

3.4. Ionic strength (I)

Through its influence on the activity factors, the ionic strength will affect the pK values of proteins. In contrast to the situation existing in a carrier ampholyte-based pH gradient, the ionic strength in a focused Immobiline pH gradient is known, and is given by the following relationship:

$$I = \sum C_{A_i} \frac{10^{(pH - pK_{A_i})}}{10^{(pH - pK_{A_i})} + 1} = \sum C_{B_i} \frac{1}{10^{(pH - pK_{B_i})} + 1} \quad (13)$$

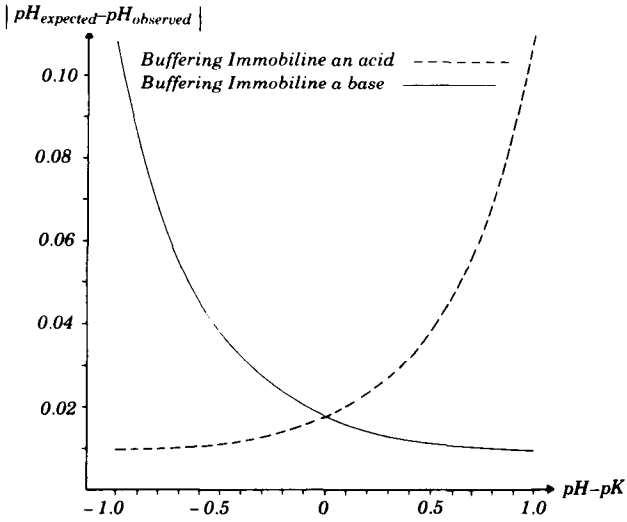

Fig. 22. Effect of a 2% error in dispensing the Immobilines on the pH of the solution, in relation to the pK of the buffering base and the buffering acid (courtesy of Dr. B. Bjellqvist; from LKB Application Note No. 321).

where C_{A_i} is the concentration of acidic Immobiline with $pK = pK_{A_i}$, and C_{B_i} is the concentration of basic Immobiline with $pK = pK_{B_i}$. It should be noted that the pK values of the Immobilines also vary with the ionic strength. From the Debye–Hückel law[32], the variation for Immobiline can be given approximately by

$$pK = pK_o - 0.5\, Z^2 \sqrt{I} \tag{14}$$

where pK_o is the pK value at an ionic strength (I) of zero and Z is equal to -1 for acids and $+1$ for bases; thus, the pK increases with I for acids, and decreases for bases. When Immobilines are used according to recommendations, these pK variations, which are less than 0.03 pH unit, can normally be neglected; however, they should be kept in mind when using extremely narrow pH gradients (approximately 0.01 pH unit/cm) or when using high Immobiline molarities (*e.g.*, 30 mM), as in these instances the band positions might be influenced.

3.5. *Buffering capacity (β)*

The β power is another quantity that is well defined in an Immobiline pH gradient. As for any solution containing weak monofunctional acids and bases, the buffering capacity is given by the equation

$$\beta = 2.3 \sum_{i=1}^{l+m} C_i \frac{K_i [H^+]}{(K_i + [H^+])^2} \tag{15}$$

where C_i is the molar concentration of the ith Immobiline having a dissociation constant of K_i. Eqns. 13 and 15, together with eqns. 7 and 8, form the core of the computer program we have described[24,25] which, given any mixture of Immobilines in any pH range, will automatically simulate and optimize the generated pH gradient together with the accompanying I and β values. With the aid of eqns. 13 and 15, the I and β power courses can also be calculated manually, usually with 0.1 pH unit increments.

The buffering capacity must be high enough to make the pH gradient insensitive to impurities (*e.g.*, acrylic acid from the acrylamide and Bis monomers) and should also be even, in order to minimize the effects of small disturbances in forming the gradient and when casting the gel[25]. For analytical purposes a β value of 5–6 mequiv. l^{-1} pH^{-1} will give pH gradients that function well. A higher buffering capacity gives more sharply focused bands[33]; however, such a gel will start to swell during the staining and destaining steps if the total molar concentration of Immobilines exceeds 30 mM.

3.6. *Conductivity*

The initial conductivity of an Immobiline pH gradient gel is determined by the amount of free, non-covalently bound ions in the gel. This is also true when the gel has been washed, as a matrix containing Immobiline will function to some extent as an ion exchanger. Thus, ions from the polymerization catalysts, and trace amounts of Immobiline, cannot be completely washed out from the gel with distilled water. When the unbound ions leave the gel, the conductivity will fall dramatically; this ion

transport can be followed visibly by refractive lines moving towards the anode and/or the cathode, marking the rear border of compounds transported towards the electrodes. If the gel initially contains large amounts of free ions, the ion transport is connected with a visible electroosmotic transport of water within the gel, resulting in the build-up of a ridge towards one of the electrodes.

With the Immobiline concentrations normally used (*ca.* 10 m*M*), the conductivity falls to values of the order of $0.2\text{–}2 \cdot 10^{-6}\ \Omega^{-1}\ \text{cm}^{-1}$ for pH gradients in the middle of the pH scale. This is about 100 times lower than the conductivity in a conventional carrier ampholyte pH gradient[13]. This extremely high resistance means that H^+ and OH^- ions start to contribute to the conductivity at around pH 5 on the acidic side and pH 9 in the basic region; below and above these values the conductivity will increase sharply. In reality this does seem to reduce the possibility of focusing in narrow gels covering a width of up to 1 pH unit even in extreme regions of pH[4]. The low absolute value of the conductivity means that there will be no "hot spots" in the gel. The stability of the gradients is also such that even proteins with a low mobility near their p*I* will have time to reach respective p*I*s in these extremely narrow pH ranges.

3.7. Electroendosmosis

Electroendosmosis is normally not a problem in Immobiline pH gradients, as the gel will not have any net charge after traces of catalysts and non-incorporated Immobilines have been electrophoretically transported away. Generally at low and high pH values the presence of H and OH^- means that the matrix adopts a net charge which will result in water transport towards the cathode at low pH and towards the anode at high pH. A trough could form close to the electrodes at the extreme pH ranges, and eventually the gel could dry out and burn. This phenomenon will in general not occur within the pH ranges for which Immobiline is recommended, but it will be wise to include glycerol (20%) in the washing step in gels below pH 5 and above pH 9.

Carbon dioxide from the air is also expected to result in electroendosmosis. Delincée and Radola[34] were the first to describe the effect of carbon dioxide. Gaseous carbon dioxide dissolves in the gel, especially at pH > 6.3 (the solubility of carbon dioxide increases with pH), forming HCO_3^- ions as follows:

$$CO_2 + H_2O \rightarrow H^+ + HCO_3^-$$

While this acidification, in conventional IEF, causes the part of the pH gradient above pH 6.3 to drift towards the cathode, by charging and mobilizing electrophoretically the focused carrier ampholytes (possibly by salt formation), it cannot act on IPGs by the same mechanism, but it will certainly alter the slope of the theoretical pH gradient depending on the local ratio $\beta(HCO_3^-)/\beta$(Immobiline) (it is in fact like introducing a new buffer with p*K* 6.3 in the immobilized pH gradient). The HCO_3^- ion migrates electrophoretically (Fig. 23) from the cathodic side towards the anode. At pH 6.3, carbon dioxide gas starts to form, and is liberated from the gel. At the same time OH^- is formed according to the equation:

$$HCO_3^- \rightarrow OH^- + CO_2\ (\text{gas})$$

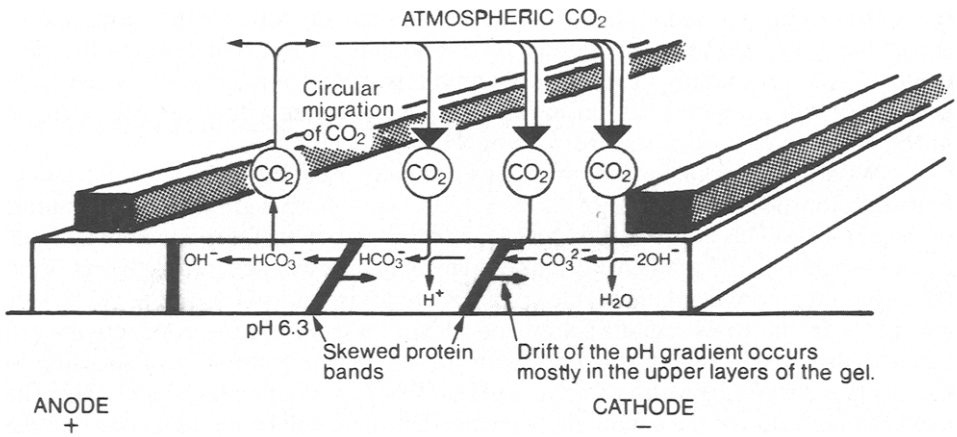

Fig. 23. Diagram illustrating the principle of interference by atmospheric carbon monoxide at high pH. Hypothetical cross-section of a gel. Note that at pH 10.3 and above, the CO_3^{2-} ion predominates, whereas between pH 6.3 and 10.3 the HCO_3^- predominates (courtesy of Dr. P. Burdett; see ref. 35).

The gas released at the anodic gel side can be re-absorbed at the cathode and thus re-circulated through the system as depicted in Fig. 23 (see ref. 35). In analogy with this, volatile amines will cause exactly the same disturbances, but in the opposite direction (it is not recommended, therefore, to use ethanolamine, ethylenediamine and the like as catholytes). Even in IPGs a very marked effect on band sharpness is observed if carbon dioxide is excluded from the system in alkaline pH ranges. For this, the IEF cell should be airtight, flushed with inert gas (denser than air, such as argon; nitrogen is lighter and will float!) and/or covered on the gel-free space with sponges impregnated with sodium hydroxide or calcium hydroxide. A note of caution should be given to scientists working with 2-D techniques: the 2-mercaptoethanol added to the sample will behave in a very similar way to carbon dioxide: it is in fact a buffer with pK 9.5. This compound ionizes at the basic gel end and is driven electrophoretically along the pH gradient. The remedy is to apply the sample at the anodic gel end: below pH 7 the -SH group will not buffer or be ionized[36].

As a final remark, we have also found a strong electroendosmotic flow when trying to cast Immobiline gels on to porous membranes for direct protein blots after the IEF step, without removal of the gel from the supporting foil[37]. We have tried several potential candidates: denitrated cellulose nitrate, cellulose acetate (including the best IEF brands), cellophane, porous polyethylene, zeta probe, Pall Biodyne; you name it: the results have been disastrous. We do not understand why IPGs should be so sensitive to porous membranes, and what exactly the mechanism underlying this electroendosmotic flow is, but at present IPGs and porous supports seem to be incompatible (Righetti, Bianchi Bosisio and Gelfi, unpublished work).

4. METHODOLOGY

In this third part I shall detail the procedure on how to cast properly an Immobiline pH gradient. This section will be purely methodological, yet its importance should not be underrated, as the quality of an Immobiline gel will be proportional

to the skills of the operator casting it. The following points will be illustrated: (a) the magnetic motor; (b) the two-chamber mixer; (c) the gel cassette; (d) gel handling after polymerization and before the electrophoretic run; (e) current, voltage and time courses in IPGs; (f) the use of additives; and (g) effects of salts and use of pH plateaux.

4.1. The magnetic motor

As stated previously (see Section 2.3), immobilized pH gradients are cast with the aid of a gradient mixer. For reproducible results, selection of a reliable magnetic drive is important. The best drive unit I have found is the IKA-WERK KMO-2 electronic, with the rheostat calibrated in revolutions per minute (500 rpm are in general adequate when the two chambers are full; half way down, the speed can be reduced to 300 rpm) (Dr. G. Peltre has also recommended to me the Vario Mag, Compact HP1, from Dr. Hoiss and partner GmbH, Munich, F.R.G.). In general, magnetic motors provided also with a thermal unit should be avoided; this kind of equipment is usually built of cheap parts and is unable to generate a constant speed: after a few minutes of operation, as the motor warms up, it increases its speed, often driving the small magnetic bars out of balance. A second important piece of practical advice: the gradient mixer sitting on top of the drive should be moved around, until the optimal position is found, *i.e.*, until the two magnetic bars (one in the mixing chamber, the other in the reservoir) rotate smoothly without irregular motions or "jumping" effects. Once the best spot is found, a piece of cardboard bearing a central hole the size of the gradient mixer should be glued to the motor casing, or the spot marked with a circle drawn on the motor cover. In this way, the gradient mixer will always be positioned in a reproducible way.

4.2. The gradient mixer

Selection of an appropriate mixing device is also critical; routinely, we use the mixer found in the LKB 2117-901 2-D and Gradient Gel kit. For reproducible mixing, the ratio of height to diameter in the chamber is critical; if the chambers are too small and narrow, the small magnets will be unable to stir the liquid column efficiently; if the chambers are too wide, and the liquid level in them is too low, the higher hydrostatic pressure of the dense solution and/or small differences in liquid heights could provoke severe remixing. The mixing apparatus described operates smoothly with liquid levels from 8.0 ml per chamber (enough to fill an entire gel cassette of 0.5 mm thickness) up to 16 ml per chamber (the required volume for filling an entire 1 mm thick cassette). The dense solution, stained with bromophenol blue, is always in the mixing chamber: as a convention, we have chosen to have the acidic (or less alkaline) part of the pH gradient in this chamber. It should be noted that the magnetic bars are present simultaneously in both vessels, although the stirring action is only needed in the mixer. If properly rotating, the two magnets will raise the liquid level in each container to the same extent, thus avoiding the generation of a differential liquid pressure owing to partial stirring in only one chamber. We prefer not to use cylindrical magnets, but prisms having as a base an equilateral triangle (12 cm high, 8 mm each side of the triangle; available from Kartell, Milan, Italy) so that they always lie flat on any of the three faces of the prism, ensuring regular and uniform stirring. Small, cylindrical bars are troublesome and should be avoided.

4.3. Preparation of the solutions

The solutions are best prepared in two 10- or 20-ml cylinders (depending on the gel thickness), labelled "dense acidic" and "light basic" solutions. Enough 30% T stock acrylamide–Bis solution is added to a concentration of 5% in the final volume of the two solutions. The acidic liquid is added with glycerol to a final concentration of 25%. Enough equivalents of buffering and titrating Immobilines are added to each vessel to generate the desired pH interval. The Immobilines should be selected and their concentration calculated according to Table 1 and nomograms I–III in LKB Application Note No. 321 (see also Figs. 9 and 10). For 2–3 pH unit wide gradients, LKB Application Note No. 322 should be consulted (see also Fig. 18 and Table 3). Once all the chemicals have been added, the solutions are brought to the desired final volume with distilled water. If the pH of the acidic and basic ends of the pH interval are now checked, it should be remembered that all calculations have been made for a run at 10°C; with the pH meter set at room temperature, the pH reading will be different from that expected at 10°C, and corrections will have to be applied, or else the pH meter calibrated at 10°C. To minimize pipetting errors, we suggest preparing at the same time 15 ml each of dense and light solutions, enough to cast two 0.5 mm thin gels (for expected errors and their magnitude, see Fig. 22).

As noted above, when casting an Immobiline gel, a superimposed density gradient is needed in order to stabilize the vertical liquid elements in the gel cassette just prior to the onset of polymerization. However, the addition of some inert chemicals such as sucrose or glycerol changes both the density and the viscosity of the solution, affecting the hydrodynamic behaviour of the gradient mixer. Ideally, the ratio η/ρ (viscosity to density) should be kept constant and as close as possible to unity. With the most common chemicals used to generate the density gradient (see Fig. 1 in ref. 24), the η/ρ ratio rapidly diverges from unity with increasing concentrations (for the 25% glycerol solution in the mixing chamber, $\eta/\rho \approx 2$). In contrast, a few inert salts, notably potasssium chloride, which can be used at concentrations lower than 10% by weight, have a fairly constant η/ρ ratio as a consequence of their effect on the water structure; thus, for highly reproducible pH gradients, I suggest to use a concentration gradient of 0–5% (or 0–10%) potassium chloride instead of the common 0–25% glycerol.

4.4. Gel cassette assembly

The gel cassette is in general assembled from few simple components. The basic units are two 3 mm thick glass slabs, one used for supporting the plastic foil on to which the gel will polymerize and the second containing a permanently glued silicone gasket, U-shaped, of 0.5 mm thickness (Fig. 24). To this cover glass one can bind up to 20 pocket-forming strips, cut out of adhesive embossing (Dymo) tape. I suggest glueing the intact length of tape and then cutting out and removing 3 mm wide segments, perpendicular to it, so as to leave glued to the glass separate rectangles of tape. The depressions formed by the Dymo tape in the gel layer are about 200 μm deep, and can usually accommodate volumes up to 10–12 μl. A double volume can be arranged for by glueing two embossing strips one on top of the other. It is always best, however, to make sure that, after opening the cassette, the pockets are sealed

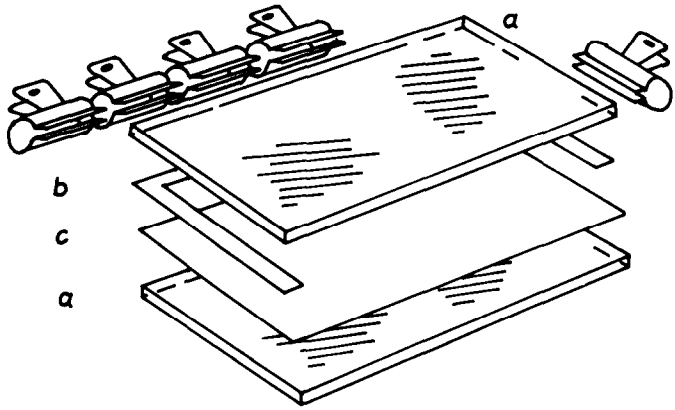

Fig. 24. Assembly of a gel cassette for casting IPGs. (a) Glass cover and base plates (3 mm thick); (b) U-gasket (in general silicone or rubber, often glued to the glass cover plate); (c) Gel Bond PAG foil, hydrophilic side up (courtesy of Dr. A. Görg; see ref. 38).

at the bottom by a thin film of polyacrylamide gel. The third component is the Gel Bond PAG film (the best brand being the light-sensitive product from FMC, Marine Colloids Division, Rockland, ME, U.S.A., which according to the manufacturer ensures a true covalent bond of the gel to the foil surface). The gel has to be supported by a plastic backing, otherwise it will tear to pieces during manipulations. Finally, we have a set of bulldog clamps for assembling the cassette and a rubber roller for smoothing the contact between the Gel Bond film and the base glass slab. The Gel Bond PAG has two unlike surfaces: one is hydrophilic for gel adherence, the other hydrophobic. A drop of water will tell them apart: it will bead up on the hydrophobic side and spread on the hydrophilic side. The hydrophilic surface should always be kept covered with the paper sheet placed in the packing between two adjacent plastic foils; one should take care not to leave fingerprints on this surface as greasy spots will repel water so that, when the gelling solution is poured into the cassette, it will distribute along their contours, leaving air bubbles in the gel. Some water is sprinkled on the short side of the 3 mm thick glass slab, and then the Gel Bond foil is lowered on to it, hydrophobic side down, and made to adhere to this surface with the help of the rubber roller. The paper foil is now removed from the plastic sheet and the surface of the latter is wiped dry of excess water with soft paper tissue. At this point, the hydrophilic surface of the Gel Bond PAG is facing the operator. The other glass slab, containing the row of pocket formers and the silicone U-gasket, should also be treated; as Immobiline gels, being charged, tend to stick to almost any surface, this last glass should be coated with a repellent. For this purpose we use LKB 1850-252 Repel Silane agent, or we simply cover the glass surface with a very thin film of vaseline (smoothed with the aid of a cotton swab). Fig. 25 shows the final assembly; notice that the two upper clamps on the top of the cassette are removed and that two paper-clips are inserted instead. This greatly facilitates the insertion of the plastic tubing conveying the solution from the mixer to the chamber, by forcing the top rims of the glass slabs to diverge and thus widen the 0.5 mm gap. The gradient mixer is positioned about 5–8 cm from the chamber top (the liquid will flow down by gravity) and is filled with the acidic and basic solutions. One should remember to fill only one

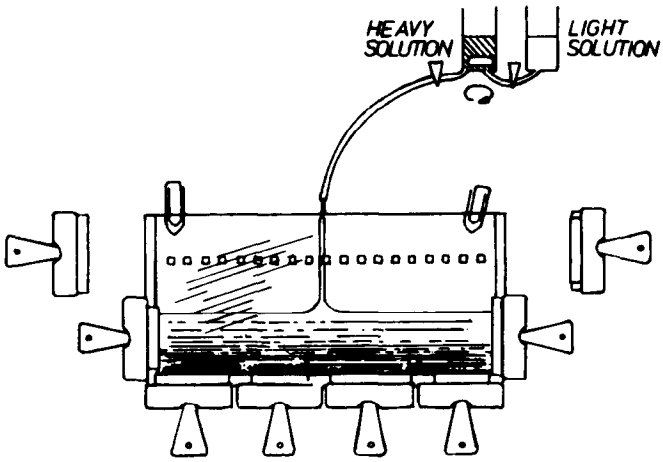

Fig. 25. Gel cassette and gradient mixer for casting an Immobiline gel. Note that the two upper clamps are removed and two paper-clips inserted instead, to widen the gap (0.5 mm) between the two glass slabs. After the gradient mixer has been emptied, the two clips are quickly removed and the clamps placed back *in situ* (the liquid level will thus rise to the proper height) (courtesy of Dr. A. Görg).

chamber first, and then to remove the air bubble from the channel connecting the two chambers by gently opening the central valve. The gel chamber is standing vertically on a levelling table and the capillary tubing is inserted in its middle. At this point the stirring is started (500 rpm), the catalysts are added (TEMED and persulphate, in this order), both valves are open and the density (and pH) gradient is allowed to flow in the gel cassette. There are *ca.* 10 min before the onset of polymerization at a temperature of 20°C, but in a hot summer (and in 8 *M* urea) things will move faster (2–3 min at > 30°C). Once the whole gradient has been poured, the clips are quickly removed and the two upper clamps fastened in their positions.

4.5. Polymerization kinetics

In copolymerization chemistry, it is often reported that the composition of the copolymer formed differs from the initial input composition because the monomers differ in reactivity towards free radical addition[39–41]. Thus, with less than 100% incorporation of monomers into the polymer, there is a possibility that the concentration ratios between the Immobilines built into the gel will differ from the ratios in the starting solution; this could have serious consequences on the pH gradient generated, *e.g.*, by changing its slope and the theoretically computed pH interval. To minimize this effect, all Immobilines are acrylamide derivatives, but even with this precaution it cannot be excluded that the resulting pH values depend to a certain extent on the polymerization efficiency. Using techniques described by Gelfi and Righetti[19,42,43] we have studied the effects of the following parameters on Immobiline gels: (a) level of persulphate, from 0.015 to 0.058%; (b) level of TEMED, from 0.024 to 0.096%; and (c) temperature range, from 20 to 60°C. The optimum polymerization efficiency (in the range 84–88% incorporation for all seven Immobilines) was found at 0.047% TEMED, 0.033% persulphate, 50°C and pH > 7. Fig. 26 gives

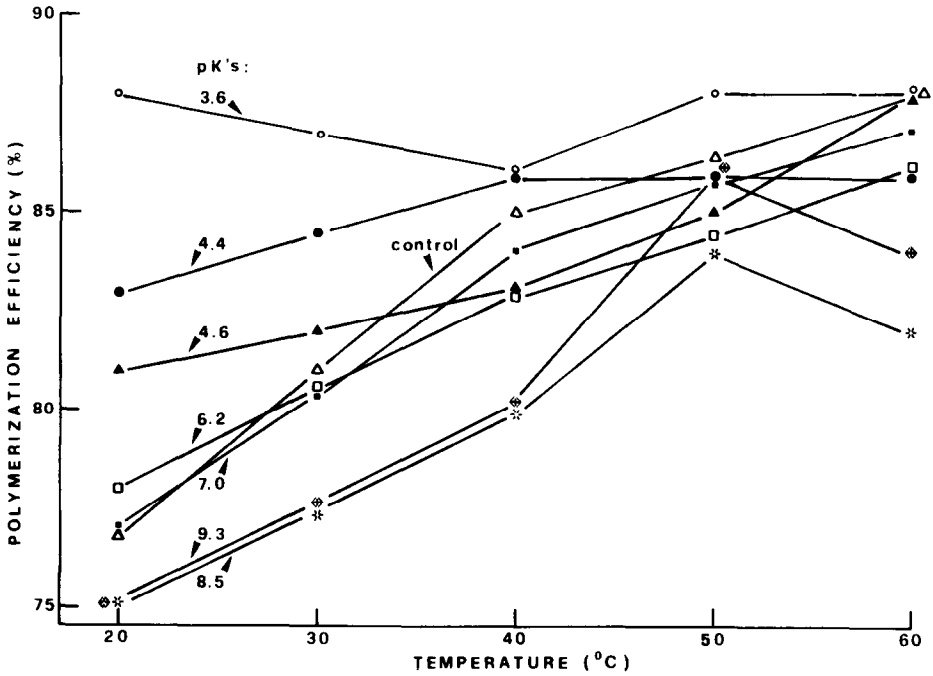

Fig. 26. Polymerization efficiency of the seven Immobiline species as a function of temperature. The percentage incorporation into the matrix is putative, as it is based on the ratio between initial and final absorbances at 285 nm (disappearance of double bonds). The best convergence (similar reactivity ratios) is only obtained at 50°C (from Righetti, Ek and Bjellqvist, unpublished work).

an example of the effect of temperature on the extent and rate of reaction of Immobilines: as the temperature is lowered, the reactivity rate diverges greatly for the different Immobiline chemicals, with a consequent lowering of the incorporation levels in the gel matrix. Curiously, at 60°C, the incorporation efficiency is lowered slightly for some species (the alkaline ones). Polymerization for 1 h at 50°C, as previously suggested, appears to be just the right solution: all Immobilines seem to come to a confluence point at this temperature, by exhibiting very similar reactivity ratios and incorporation efficiency (Righetti, Ek and Bjellqvist, to be published). Another important lesson has been learned from these experiments: when casting extended pH gradients (*e.g.*, pH 3.5–9.5, the widest possible with Immobiline chemicals) it is imperative that the acidic end of the pH gradient be titrated (with sodium hydroxide solution) at least around pH 8, so as to ensure a uniform reactivity ratio between the two pH extremes.

When Immobiline gradients are cast as shown in Fig. 25, with a gradient mixer equilibrated in air, an 84–88% incorporation efficiency is the best that can be achieved, and this for most practical applications will be adequate. However, if better than 96% incorporation is required for some special experiments, this can be achieved by completely excluding oxygen from the polymerization mixture. We have achieved this by building a gradient mixer that provides for anaerobic conditions, but the experimental manipulations become more complex.

4.6. Gel handling after polymerization

After standard polymerization (1 h, 50°C) the gel cassette is removed from the oven, the eight clamps removed and the supporting glass plate gently pried open with the tip of a spatula. The Gel Bond PAG foil can now be lifted from one corner and gently peeled off, with the bound polyacrylamide gel layer, from the other glass plate closing the cassette. The first operation to perform at this point is a weighing step (after blotting any traces of liquid around the ridges of the foil, if needed), as the gel has to be washed and will swell in water during this procedure. It is a good idea to mark the weight of the gel on the plastic backing. The gel is now washed in 1 l of distilled water for 30–40 min for 0.5 mm thick gels (for double this time for 1 mm gels). The washing step is essential: TEMED, persulphate and 12–16% unpolymerized Immobilines have to be removed, otherwise huge plateaux of free acid and free base will form at anode and cathode, respectively, and will prevent the protein from focusing. After washing, the gel should be blotted with soft tissue and then, with the aid of a fan, reduced to its original weight. This step is essential, as gels containing too much water will "sweat" during the IEF run and droplets of water will form on the surface. It is at this point that (if you have not quit in despair owing the many manipulations involved) you can apply your sample. There are different ways of doing it: with Paratex tissue pieces or with a surface template containing holes of different size and shape. I still prefer, however, to load the sample in a free liquid form in a pocket pre-cast in the gel.

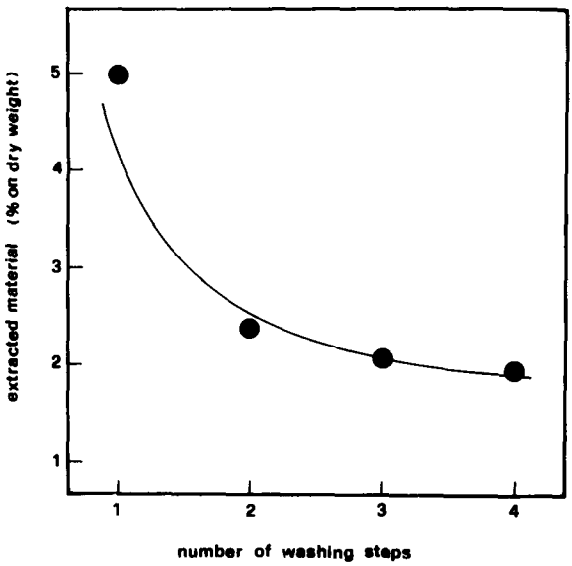

Fig. 27. Efficacy of repeated washing steps on the reduction of extractable material from IPGs. IPGs in the pH range 5.4–6.4 were washed in distilled water (500 ml per 10 ml of gel) 1–4 times, 30 min each. The gel was then extracted with 80% acetic acid and the supernatant dried to constant weight on potassium hydroxide (from Gianazza *et al.*; see ref. 18).

4.7. Gel drying and storage

It is not a problem to dry the standard, 5% T, 4% C, 0.5 mm thick gels for subsequent use. They should, however, be washed prior to storage, as this enhances the stability of the dried gel (Gianazza and Righetti, unpublished work). From this point of view, two or three consecutive washings are even better, as they greatly diminish the amount of extractable material from the gel (including shorter or longer uncross-linked polyacrylamide segments; see Fig. 27). Nothing is gained by continuing the washings after the third. The gels should be thoroughly desiccated, as with traces of water slow hydrolysis of the amide bonds will continue even at 4°C, expecially at the alkaline end, and therefore glycerol should be eliminated from the washing solutions (it is customary to dry gels after equilibration in 3–5% glycerol). After drying, the gel surface is covered with Parafilm, then, while lying on a thick glass plate, wrapped around with Saran wrap and stored at 4°C in a desiccator. We have stored gels in this way for at least 1 month and have experienced only some blurring of the bands at the very alkaline gel end (pH > 9). Re-swelling prior to use in general is performed for a few hours up to overnight (depending on gel thickness). Conditions have been described for re-swelling in the presence of urea[44], but this should not be attempted with detergents as the high viscosity of the solution and the large micelle size prevent proper equilibration even for periods of several days (Righetti, unpublished work).

4.8. Electrolyte solutions or not?

In the first work on the method[4,18,24,25] we did not use any electrolyte solutions soaked in filter-paper strips, as is done in conventional IEF, the platinum wires being in direct contact with the gel surface. It is now recommended (see LKB Application Note No. 322) to use 10 m*M* glutamic acid at the anode and 10 m*M* sodium hydroxide solution at the cathode. Although for the IPG separation process *per se* electrolyte strips are not needed, there are at least two good reasons for using them: (a) with the advent of the Macrodrive (5 kV) it could be dangerous to use such a high voltage with the platinum wires only 0.7 mm away from the surface of the cooling plate; on humid summer days there is a great danger of short-circuits and sparks between the two electrodes with a risk of destroying the IEF chamber (this has indeed happened; Dr. B. Bjellqvist, personal communication); the electrolyte strips will keep the platinum wires several millimetres above the plate surface; (b) when applying the sample at the anodic side, products with a high oxidizing power are released from the anode and diffuse into the pocket, modifying the protein (this happens within a few minutes after applying the voltage; I have seen haemoglobin turn brown instantly!). In presence of electrolyte strips this process is greatly slowed down (possibly because these products are absorbed by the paper, or because of the pH in the strip or because gel components take a longer time to diffuse through the paper and touch the platinum wire), so that the sample has time to move out of reach of these oxidizing products. Another case in which electrolyte strips are recommended is when using highly diluted (and thus soft) gels for preparative runs (see Section 5.6).

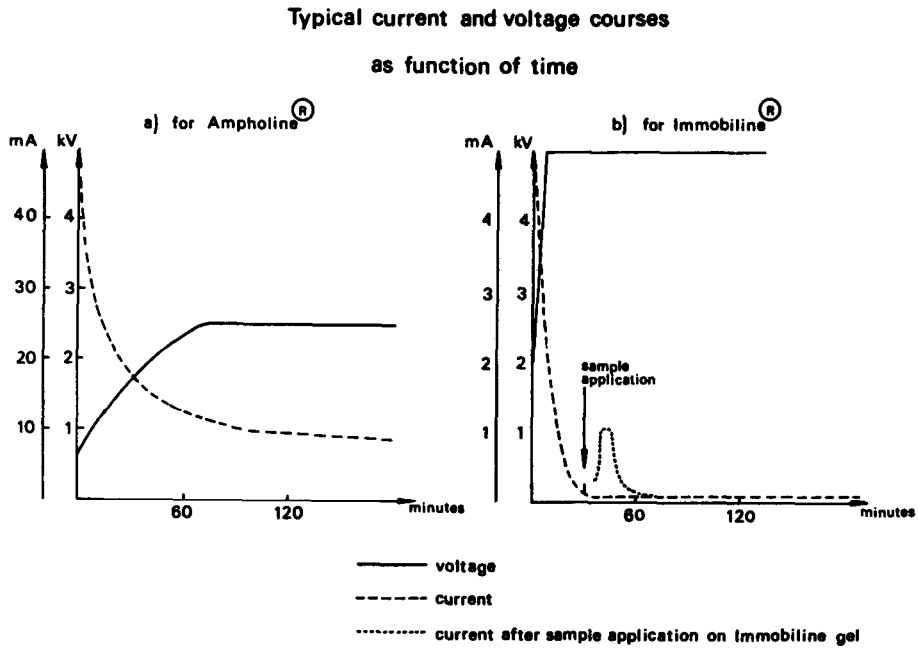

Fig. 28. Current and voltage courses in (a) Ampholine (left) and (b) IPG gels (right). The broken line represents the extra current generated in pre-run IPG gels after sample application (courtesy of Dr. B. Bjellqvist).

4.9. Current and voltage courses in IPGs vs. CA gels

Just to keep faith with what I have stated above (see Section 3.6), we can compare the electrical conditions in CA gels with Immobiline matrices. As shown in Fig. 28a, in CA gels under steady-state conditions the current drops to a minimum of the order of *ca.* 5–10 mA, while the voltage reaches a plateau at 2500 V, giving a total wattage in the range 12.5–25 W. These plateau values are usually reached in *ca.* 45 min after starting the experiment. In IPGs, the conditions are dramatically different: within 5–10 min the current has dropped to values of the order of microamperes, and the voltage is proportionally increased to whatever values the power supply can reach (5000 V, as generated by the LKB Macrodrive, is surely an excellent voltage drop to have!). Rarely the wattage conditions exceed 1 W, so that there are practically no temperature gradients within the gel thickness. In theory, if available, and with due precautions, one could apply as much as 10,000 V/cm, which is the safety limit before a spark discharge in air (12–15 kV, depending on humidity conditions; definitely off-limits in the tropics). At these voltage gradients, even the laziest, siesta-prone proteins had better speed up. A temporary, small increase in current is experienced when the sample is applied (see arrow in Fig. 28b).

4.10. Time scales in IPGs

As shown in Table 4, the experimental time in IPGs depends on two basic

TABLE 4

TIME SCALES IN IMMOBILIZED pH GRADIENTS

Modified from LKB Application Note No. 322. I have omitted the column on pre-run as I believe that Immobiline gels should never be pre-run (if the salt front moves without the sample the residence time of the protein in the application pocket will be too long and there will be a great risk of protein denaturation).

Width of pH gradient (pH units)	*Run time with LKB Power Supply*	
	*2197**	*2297***
0.5	Overnight	Overnight
1	Overnight	Overnight
2	Overnight	4 h
3	4 h	2 h

* Set at maxima of 2500 V, 5 W and 25 mA.
** Set at maxima of 5000 V, 5 W and 2500 mA.

parameters: the width of the pH gradient and the available field strength. For narrow and ultra-narrow pH gradients (< 1 pH unit) focusing should continue overnight with any power supply (2.5 or 5 kV). This is because the proteins are already in a portion of their titration curve close to their p*I* position, where, in several cases, the d*u*/d(pH) value is small, and therefore long times are required to slow-moving protein ions to reach their p*I* values. The situation is moreover aggravated by the low conductivity of Immobiline matrices, which further impedes migration of macro-ions to their equilibrium position. However, in wider pH gradients (2, 3 up to 6 pH units) the migration of the protein ions will be much faster and here the potential differential will also play an important role; essentially, doubling the voltage drop results in halving the focusing times.

4.11. Additives

The most common additives, especially in work with 2-D maps, are 8 *M* urea and 2% neutral detergent (Nonidet P-40 or Triton X-100) either singly or in a mixture. Owing to their influence on hydrogen ion activity (disruption of the water structure by the chaotrope urea, seclusion from the detergent micelles) these agents are likely to influence the p*K* of Immobiline buffers and thus modify the theoretically predicted pH range. As shown in Fig. 29, this effect is pronounced in 8 *M* urea; interestingly the ΔpK [p*K* (urea) − p*K* (H_2O)] is high for acidic Immobilines (0.9 pH unit for p*K* 3.6) and progressively lower for the alkaline species, down to only 0.42 pH unit for the p*K* 9.3 species. The new p*K* values, measured at 20°C, in 8 *M* urea are as follows: p*K* 3.6, 4.46; p*K* 4.4, 5.21; p*K* 4.6, 5.48; p*K* 6.2, 6.81; p*K* 7.0, 7.48; p*K* 8.5, 9.13; and p*K* 9.3, 9.84. When running extended pH gradients (4–6 pH units) in 8 *M* urea some special precautions have to be adopted: either the gel (polymerized in the presence of urea) is pre-run overnight, perpendicularly to the direction of the pH gradient, and then the anodic and cathodic edges are excised (this effectively removes unbound ions, but reduces to 60–70% the gel surface available for sample fractionation) or the gel (cast in the absence of urea) is thoroughly washed (2–3 times), dried and re-swollen in urea solutions[44].

Conversely, the effect of 2% Nonidet P-40 on Immobiline p*K*s is small; it is

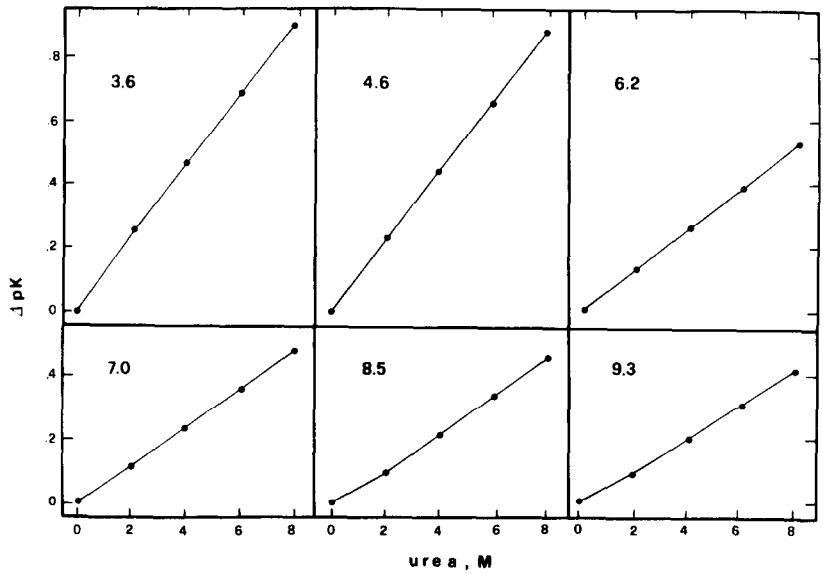

Fig. 29. Dependence of Immobiline p*K*s on urea concentration. A 20 m*M* solution of each Immobiline was titrated to its p*K* (with Immobiline of p*K* 3.6 or 9.3 as counter ion). Aliquots of this stock solution were diluted to a 10 m*M* concentration in the presence of various amounts of urea. pH readings were made at 20°C. ΔpK refers to $pK_{urea} - pK_{water}$ (from Gianazza *et al.*; see ref. 44).

virtually negligible for tertiary amine species (of the order of 0.01 pH unit) and slightly larger for the acidic compounds (up to 0.08 pH unit for the p*K* 3.6 Immobiline). This is comforting, and suggests that acidic and basic Immobilines have little tendency to conglomerate into detergent micelles, unlike conventional carrier ampholytes, which form mixed micelles with neutral detergents[45]. Moreover, unlike in urea solutions, the behaviour of acidic and basic Immobilines in detergents is monotonic; both species become weaker acids and weaker bases, respectively, which means a p*K* increase for the acids and a p*K* decrease for the bases (see Fig. 6 in ref. 44; however, note that although the legend to Fig. 6 is correct, two diagrams have been transposed and the diagram in Fig. 5 should be consulted).

4.12. Effects of salts, pH plateaux

In conventional IEF, the carrier ampholytes are relatively free to move within the gel matrix, even when standing at their p*I* position, so that they are liable to disturbances by salt ions transported through the gel. The mechanism of pH gradient distortion and concomitant "wavy" protein bands due to the presence of salts and/or weak electrolytes in the samples are not completely understood but seem to be due, according to recent theories[46], to the generation of a second pH gradient, perpendicular to the direction of the original one established by the IEF process *per se*. As a result, the p*I*-standing carrier ampholytes are titrated, acquire a net charge and move electrophoretically to a new position in the IEF column (or plate). On the other hand, IPGs, being covalently bound to the gel matrix, are in principle unaffected by salt ions. There are, however, some practical limits to the amount of salt that can be tolerated even in IPGs, and they are due to (a) initial conductivity of the IPG gel;

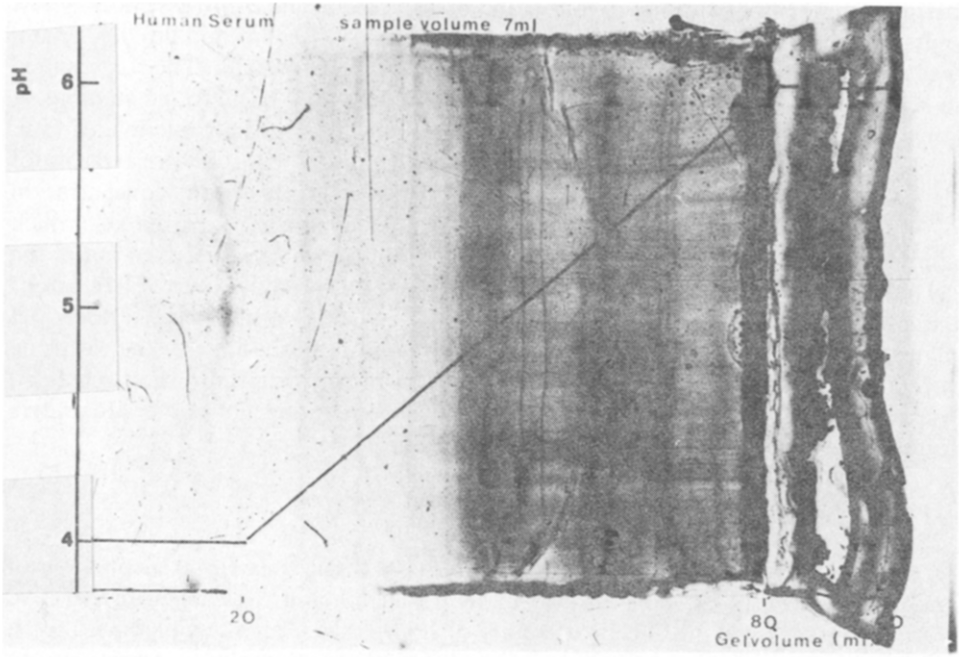

Fig. 30. IEF of undialysed human serum. The IPG was modified to contain two pH plateaux at the ends of the pH gradient, comprising either the acidic or the basic pH and Immobiline composition used to generate the pH gradient 4–6. During sample application the electrodes were placed at the ends of the gel, then serum was applied batchwise, 1 ml at a time. When the salt had migrated out of the system and visibly concentrated at the anode, the two electrodes were moved inwards to the two extreme ends of the pH gradient to use the applied field strength over the gradient efficiently and thus maintain maximum resolution (from Ek *et al.*; see ref. 47).

(b) generation of strongly acidic and strongly basic gel zones in the proximity of the electrodes as a consequence of the physical separation of the salt ions. With respect to the first point, different amounts of salts can be tolerated in different pH ranges: at acidic pH (3.5 – 5) as much as 10–15 μmole of sodium chloride per ml of gel solution can be tolerated by the system, the corresponding amount in the pH range 9–10 being 3–4 μmole/ml (it should be remembered that the free proton mobility is 350 $cm^2\ V^{-1}\ sec^{-1}$ while the corresponding OH^- mobility is only 85 $cm^2\ V^{-1}\ sec^{-1}$ at 25°C). However, in the pH range 5.5–9, where the conductivity of the system is at a minimum, and the contribution of free H^+ and OH^- is small, the maximum tolerable amount is barely 0.5 μmole/ml.

The second problem (collection of free cations and anions at the two electrodes, with formation of plateaux with extreme pH values) can be solved by elongating the gel with pH plateaux at the two extremes, where the ion components of the salt can collect just outside the Immobiline pH gradient. How this is done is shown in Fig. 30. Here a gel with dimensions 150 × 110 × 5 mm has been cast in the LKB 90001157 glass tray standing on one end. First the mould is injected with 20 ml of a "cushion" solution (40% glycerol, constant pH = 4) to give one pH plateau, and on top of that is cast an Immobiline pH 4–6 gradient with a length of 10 cm, containing a 25–5% glycerol density gradient. On top of this is gently floated a second

pH plateau (20 ml of constant pH = 6 and 0% glycerol). The entire assembly is now polymerized in the oven at 50°C for 90 min. A volume of 7 ml of non-desalted serum was applied batchwise, corresponding to about 500 mg of protein. The run resulted in separated protein bands, free of distortion and with little background staining. A conventional carrier ampholyte-based gel would have been heavily overloaded even at a lower sample load (in the experiment described here, the buffering capacity of the gel has been increased up to 12 mequiv. $pH^{-1}\ l^{-1}$ by increasing the concentration of Immobiline. This also increases the background conductivity of the gel, which allows it to tolerate higher salt loads and means that the salt is also driven out of the gel more quickly[20,47]. In general, once we have seen the refractive lines of free anions and cations moving out of the separation gel and collecting at the two electrodic pH plateaux, we physically remove them by excision and re-positioning of the electrode wires. This method can also be used for removal of salt from unwashed gels (*e.g.*, because they contain expensive additives; see the preceding section) as an alternative to the "lateral excision" technique of Gianazza *et al.*[44].

5. PREPARATIVE APPLICATIONS

I shall explore here the preparative aspects of IPGs; since their inception as an analytical technique, it soon turned out that their loading capacity in preparative work was just as striking. The load ability of IPG gels has been demonstrated to be at least ten times higher than in conventional IEF, thus approaching or even passing the load limit of isotachophoresis[33,47]. The following aspects will be discussed: (a) explorative runs aimed at defining the load capacity; (b) optimization of experimental parameters (I, pH gradient width, gel thickness); (c) protein detection by refractive index variations; (d) protein recovery from Immobiline gels and elution from hydroxyapatite beads; and (e) protein load as a function of %T in the matrix.

5.1. Theoretical prediction of acceptable protein loads in IPGs

For practical preparative work an equation has been derived correlating the maximum protein load in a single zone to the pI distance (ΔpI) with the nearest contaminant, to the gel cross-sectional area and to the slope of the pH gradient. The equation is

$$M = \left[\frac{\Delta \mathrm{p}I}{\mathrm{d(pH)}/\mathrm{d}x} - L\right] \cdot 2C_{\mathrm{M}}\, A \tag{16}$$

where M = protein load in a single zone (major component) in mg; ΔpI = pI difference between major component and nearest contaminant (in pH units); d(pH)/dx = slope of the pH gradient along the separation track (pH units/cm); L = protein-free space, between the major band and the impurity, which is needed to cut the gel without loss of protein or without carrying over the impurity (in general 1 mm is an acceptable distance); C_{M} = average concentration in the focused zone of the major component (mg/ml); and A = cross-sectional area of the gel perpendicular to the focusing direction (in cm^2).

It can be seen that protein load can be maximized by increasing A (the liquid

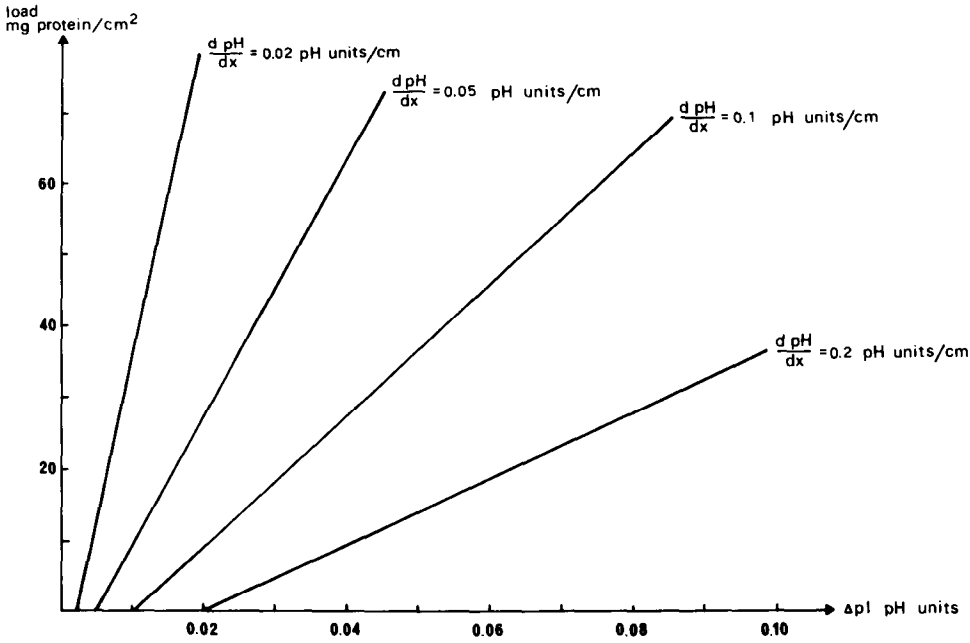

Fig. 31. Acceptable protein load as a function of ΔpI for different pH slopes plotted for a mean concentration of 45 mg/ml in the major protein zone. This is a graphical representation of eqn. 16 (from Ek *et al.*; see ref. 47).

volume available to the focused zone) and by decreasing the slope of the pH gradient (*i.e.*, by focusing in ultra-narrow pH gradients). As a practical guideline, a graph has been constructed correlating these three basic experimental parameters: protein load in a single zone, ΔpI between the band of interest and nearest contaminant and slope of the pH gradient along the separation axis [d(pH)/dx]. This graph is essentially a plot of eqn. 16, taking as a concentration limit (C_M) a common upper limit, found experimentally, of 45 mg/ml. Fig. 31 shows how the graph is laid out: the abscissa reports the ΔpI value (in pH units) and the ordinate the protein load (mg/cm²) for a given A value. The ΔpI *vs.* protein load plane is cut by lines of different slopes, representing pH gradients of different widths along the IPG gel length. It is seen that ultra-narrow pH gradients (*e.g.*, 0.02 pH unit/cm) allow extremely high protein loads (up to 80 mg/cm²) while still retaining a resolution better than $\Delta pI = 0.01$. At the opposite extreme, broad pH gradients (*e.g.*, 0.2 pH unit/cm) would allow a resolution of only $\Delta pI = 0.1$ with a protein load of less than 40 mg/cm².

5.2. *Optimization of environmental parameters*

We have also performed a thorough study of the optimization of environmental parameters (I, gel thickness, pH gradient width) for maximizing protein loads in immobiline matrices[48]. These aspects are summarized in Fig. 32. By increasing the ionic strength of the gel from 1.25 to 7.5 mequiv. l^{-1} a 4-fold increment in load capacity is obtained; above this level, a plateau is abruptly reached around 10–12 mequiv. l^{-1}. By increasing the gel thickness from 1 to 5 mm a proportional 5-fold increment in

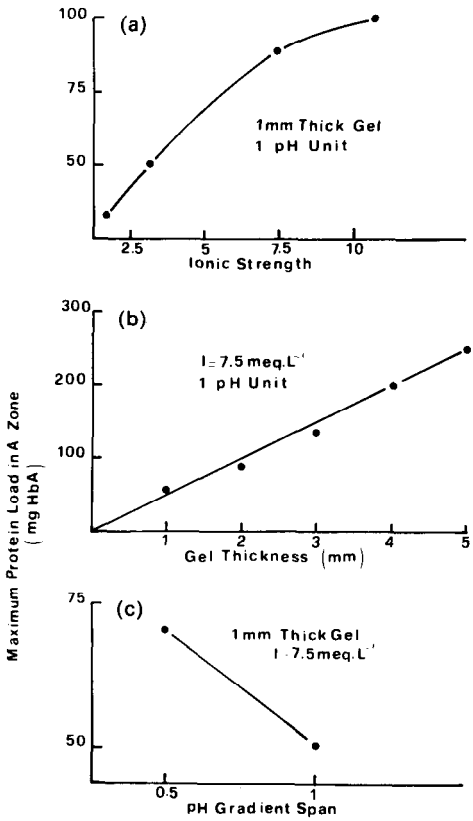

Fig. 32. Loading capacity of IPGs. The maximum load in a single protein zone is plotted (a) as a function of ionic strength at constant gel thickness (1 mm) in a 1 pH unit span, (b) as a function of gel thickness at constant ionic strength in a 1 pH unit interval and (c) as a function of pH gradient width at constant ionic strength and constant gel thickness (from Gelfi and Righetti, unpublished work).

protein load ability is achieved; the system does not level off, but a 5 mm thickness seems to be optimal as thicker gels begin to develop thermal gradients in their transverse section, generating skewed zones. Finally, by progressively decreasing the width of the pH interval, there is a linear increase in protein load capability; here too the system does not reach a plateau; however, owing to the very long focusing times required by narrow pH gradients, aggravated by the high viscosity of protein zones at high loads, it is suggested not to attempt to fractionate large protein amounts in pH ranges narrower than 0.5 pH unit.

We have seen in the above section that IPGs have a load ability at least ten times higher than conventional IEF. I believe this is mostly due to the strong difference in ionic strength characteristic of the two systems. At a very low I values typical of IEF (*ca.* 1 mequiv. l^{-1}) macromolecules will have a very low solubility minimum, and will tend to aggregate and flocculate. An increase in I, *ca.* 7–10 mequiv. l^{-1} as characteristic of IPGs, is thus beneficial because, according to the Debye–Hückel equation:

$$-\log \gamma = \log (S/S_o) = 0.51\, Z^2 \sqrt{I} \qquad (17)$$

where γ is the activity coefficient of an ion of charge Z and S and S_o are the solubilities of a protein at the pI at a given ionic strength and as extrapolated to zero ionic strength, respectively. Thus, as the environmental I increases, and the γ values of the ions (both in solution and in the protein) decrease, the protein solubility increases; this is the well known "salting-in" effect described in 1936 by Cohn[49]. I am tempted to equate IPG gels to "salting-in" media and IEF gels to "salting-out" milieux. It might be argued that, as long as the proteins precipitate at their pI, and this material is confined in the isoelectric zone, this should not affect the load capacity in gel matrices, as the precipitated zone is gravitationally stable. The point is that in real cases this does not happen. As demonstrated by Gronwall[50], the solubility of an isoionic protein, plotted against pH near the isoionic point, is a parabola, with a fairly narrow minimum at relatively high I, but with progressively wider minima, on the pH axis, at decreasing I values. We have re-plotted his data in Fig. 33: it can be seen that, at the prevailing Is typical of conventional IEF (1 mequiv. l^{-1}), the solubility minimum of β-lactoglobulin spans at least a 0.3 pH unit interval, whereas in IPGs (I = 10 mequiv. charges l^{-1}) the pH of solubility minima is strongly decreased in a funnel-shaped fashion down to only 0.05 pH unit. In other words, what is detrimental in preparative IEF runs *is not isoelectric precipitation, but near-isoelectric precipitation. The precipitate is not confined at the pI position, but is usually spread over as much as 1/2 pH unit interval*, thus being completely detrimental to the resolution of adjacent species.

5.3. Protein detection

Let us now progress into the practical aspects of preparative IPG runs. At the end of a separation, we have first to reveal the focused protein zones in order to

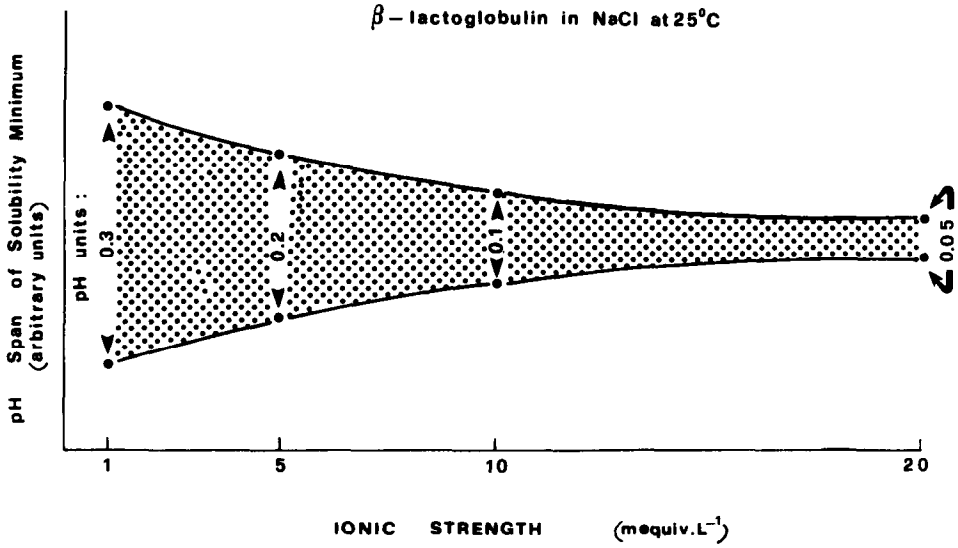

Fig. 33. Solubility of a protein in the neighbourhood of its pI as a function of the ionic strength of the milieu. At 1 mequiv. l^{-1} (conditions prevailing in conventional IEF), β-lactoglobulin has a minimum solubility over a span of 0.3 pH unit; the width of the solubility funnel is markedly decreased at high I values (it is only 0.05 pH unit at 10 mequiv. l^{-1}, a value typical of an IPG milieu) (from Gelfi and Righetti; see ref. 33).

excise and elute the band of interest. In IPGs, this can be done in two ways: by Coomassie staining or by visual inspection of refractive indices. In the former instance, at the end of the IPG run, a strip is cut from each edge of the gel, parallel to the pH gradient and including part of the area where the sample was applied. The two strips are then fixed and stained so as to reveal the protein zones, while the gel slab is kept under voltage (this can be done as there is no cathodic drift, so the band position does not change with time). By putting the now stained gel strips back into their original position, the protein zone of interest is located and the gel strip containing it is cut out. Even more interesting is the second detection method: as discovered long ago by Kolin[2], in his "artificial" pH gradients obtained by buffer diffusion, a protein zone condensed at its p*I* will exhibit a sufficiently steep refractive index gradient to be detected by the naked eye. This clever detection principle is lost in conventional IEF, however, as the carrier ampholytes themselves, once focused at their p*I* under high voltage, would give a very complex striation pattern[51], thus completely obscuring the protein position. This principle is again fully operative in Immobiline gels, as the buffering species cannot collect in ridges about their p*I*; as shown in Fig. 34, the focused ovalbumin zones are clearly visible as refractive lines, the detection limit being possibly as low as 5–10 μg per band. Hence this detection principle can be substituted as a guideline for detecting and cutting the protein zone of interest without resorting to Coomassie staining.

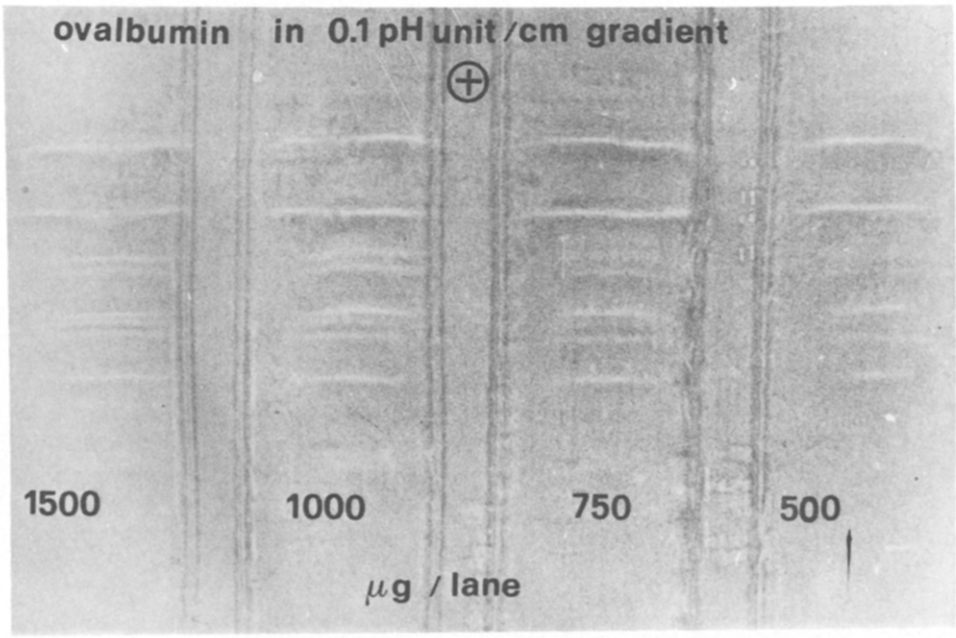

Fig. 34. Detection of unstained protein zones in Immobiline gels by refractive index gradients. Ovalbumin (sample load shown under each track) loaded in slots at the cathode in 0.5 mm thick gels in an immobilized pH 4.2 5.2 gradient. Focusing: overnight at 2000 V, 10°C. The gel was photographed directly after switching off the voltage with a shallow side illumination (from Ek *et al.*; see ref. 47).

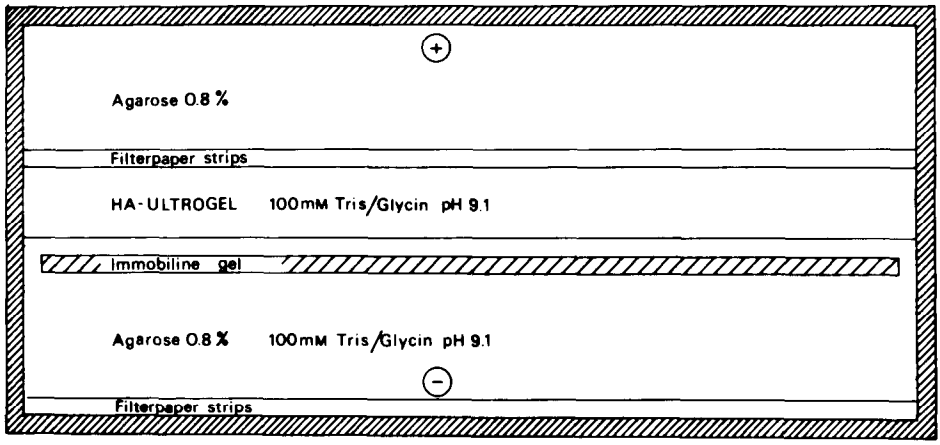

Fig. 35. Recovery of protein zones from Immobiline gels. Application of the polyacrylamide gel strip from the first step to the agarose gel of the second step. The polyacrylamide gel strip, containing the protein of interest, is cut along the contours of the main band (still supported by the Gel Bond PAG). The 0.8% agarose gel layer, 5 mm thick, was made to contain 100 m*M* Tris–glycine buffer (pH 9.1). A trough was cut in the agarose gel to accommodate the polyacrylamide gel strip with a snug fit. The protein is recovered in the beads of hydroxyapatite contained in the central trough by applying a constant power of 30 W for 60 min (420 V initial voltage drop) at 10°C (from Ek *et al.*; see ref. 47).

5.4. Electrophoretic protein recovery in composite agarose–hydroxyapatite (HA) gels

As IPGs can behave as ion-exchange matrices, protein recovery is performed electrophoretically. This step consists in the electrophoretic transport of the focused protein zone out of the IPG gel strip into a layer of hydroxyapatite-containing granulated gel, through a contact made of an agarose bed[52,53]. Electrophoresis is performed in an LKB 90000157 glass tray, of dimensions 245 × 120 × 5 mm (see Fig. 35). Three LKB 1850-911 electrofocusing strips, soaked in 100 m*M* Tris–Gly buffer, pH 9.1, and cut to length, are placed one on top of the other against the silicone rubber frame at the cathodic long side of the tray; three more strips, likewise treated, are placed 40 mm from and parallel to the anodic long side of the tray. Molten 0.8% agarose-M, in 100 m*M* Tris–Gly buffer (pH 9.1), is poured into the tray and allowed to set. A 20 mm wide agarose strip is then removed along the anodic filter-paper strip and replaced with a slurry of HA Ultrogel (crystals of calcium phosphate coated with agarose). The IPG gel strip, containing the protein of interest, is now placed 5 mm away from and on the cathodic side of the HA Ultrogel. If the IPG gel strip is 0.5–1 mm thick, it can simply be laid on top of the agarose gel (with the gel side facing down and the Gel Bond PAG facing the operator). For 2–5 mm thick gels, the protein-containing IPG strip is placed in a trough of the same size cut out of the agarose gel layer, having a corresponding 2–5 mm thickness: this ensures uniform electrophoretic transport throughout the thickness of the IPG gel strip. The electric circuit is now closed with paper wicks going from the electrolyte reservoir of the Multiphor chamber to the surface of the agarose gel. The electrode buffer is 0.2 *M* Tris–Gly (pH 9.1) and the electrophoretic removal is performed at 30 W constant power for 1 h at 10°C with an initial voltage of 420 V. As shown by Coomassie Blue staining, almost no protein remains behind in the IPG gel strip.

The HA beads are prepared as follows. They are first washed once, in a Büchner funnel, under suction, with 1 *M* phosphate (pH 6.8) (100 ml of buffer per 10 g of gel), to remove any traces of contaminant proteins from previous experiments. Thereafter they are washed, still under vacuum, with 1 l of distilled water, transferred into a beaker and equilibrated in 100 m*M* Tris–Gly buffer (pH 9.1). The gel slurry is again transferred to a Büchner funnel and carried to a consistency that would allow the HA beads to be applied directly with a spatula to the trench in the agarose gel. There are at least two good reasons for preferring electrophoretic elution to diffusional recovery from ground gel pieces: the IPG matrix, once finely ground, would swell considerably in the elution buffer (thus re-absorbing the protein) and it would release in the supernatant uncross-linked polyacrylamide Immobiline chains (thus contaminating the sample)[18].

5.5. Protein elution from HA beads

After electrophoresis, the HA Ultrogel is transferred with a spatula to a 25-ml plastic syringe plugged in the bottom with some cotton-wool or with discs of filter-paper. The protein is eluted with aliquots of 0.2–0.25 *M* phosphate buffer (pH 6.8). In addition to the first fraction, 5 × 7 ml of buffer are normally sufficient to remove all the protein from the HA gel. The buffer aliquots are pipetted in the syringe barrel, the beads briefly stirred with a glass rod and then the buffer is eluted in a test-tube with the aid of the syringe piston; this helps to squeeze out all the liquid from the HA crystals. The HA beads can then be regenerated for subsequent use by washing in 1 *M* phosphate (pH 6.8) as described above.

The recovery from HA beads has been tested for six different proteins: haemoglobin (Hb), myoglobin, bovine serum albumin (BSA), carbonic anhydrase, ovalbumin and human transferrin. Recoveries ranged from 76% (BSA) to 98% (Hb and myoglobin), typical values being of the order of 85%. These yields from Immobiline

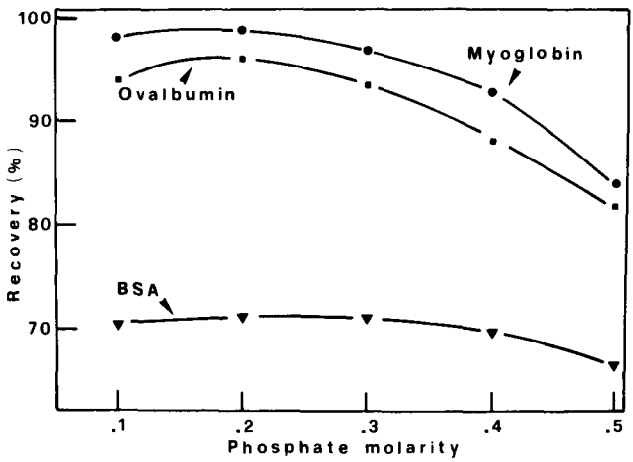

Fig. 36. Recovery of protein fraction as a function of phosphate eluent molarity. Myoglobin (●), ovalbumin (■) and BSA (▼) were separately absorbed on HA-Ultrogel, equilibrated in 100 m*M* Tris–glycine buffer (pH 9.1) and eluted with increasing molarities (from 0.1 to 0.5 *M*) of pH 6.8 phosphate buffer (from Ek *et al.*; see ref. 47).

matrices are of the same order of magnitude as protein recoveries from Sephadex beads run in conventional IEF by the Radola technique[54]. Recoveries are optimized by working in a range of 0.2–0.25 *M* phosphate concentrations (see Fig. 36); at lower (0.1 *M*) and higher values (0.5 *M*) there is a loss of protein, in the former instance due to ion bonding and in the latter probably due to hydrophobic interaction with the HA matrix[55].

5.6. Protein load as a function of %T

It turns out that the situation, in preparative runs, is more complex than I have described. We have seen (Section 5.1) that, no matter how the experimental conditions are optimized, and the ionic strength is increased (see Section 5.2) a common upper load limit for all proteins investigated has been found, of 40–45 mg of protein per ml of gel solution. We have been intrigued by this barrier and have tried to carry our IPG–Concorde plane through this "sound wall". The key to this apparent "solubility limit" can be found in Fig. 37: the amount of protein accepted by a gel matrix is directly related to its composition (%T). The limit of 40 mg of protein per ml of gel is only valid for a 5% T polyacrylamide matrix: as the amount of fibres in the gel is decreased, progressively more protein can be loaded in the system, so that in a 2.5% T gel as much as 90 mg of protein per ml of gel can be applied. This has been interpreted as a competition for the available water between the two polymers, the polyacrylamide coils and the protein to be fractionated. This is an extraordinary amount of material to be carried by a gel phase, and renders IPG by far the leading technique in any electrophoretic fractionation. However, such soft gels are difficult to handle; for easier manipulations, we have described a two-step casting procedure, based on the formation of a %T step and a pH plateau around the application trench

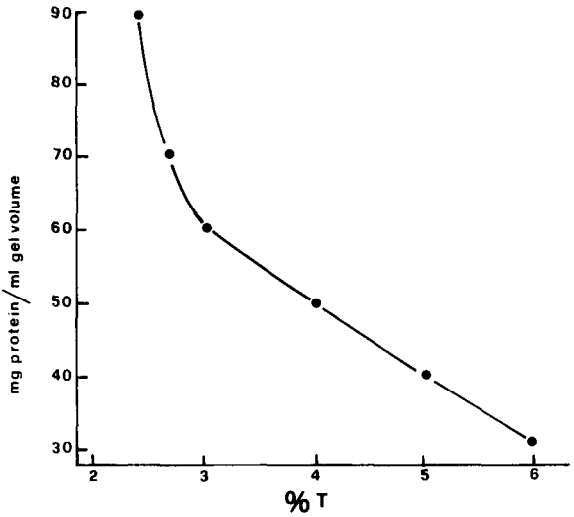

Fig. 37. Relationship between loading capacity (in terms of mg of protein per ml of gel volume) and %T value (T = grams of acrylamide and cross-linker per 100 ml gel volume) of the gel matrix. Notice that, whereas in the range 3–6% T the protein load decreases linearly, in softer gels (<3%T) it increases exponentially (from Righetti and Gelfi; see ref. 20).

(to prevent collapse of the trench walls and to speed up the electrophoretic migration of the protein out of the application zone) (for casting a gel with plateaux, see Section 4.12). We have also described a new method for electrophoretic recovery from IPG gel strips, based on embedding on low gelling (37°C) agarose instead of forcing the IPG strip into a trench cut into a pre-gelled agarose layer (see Section 5.4)[20].

5.7. The 1-g protein load: altimetric gel profile

The highly diluted gels we have described above have two additional advantages: (a) by diluting the matrix, while keeping constant the amount of Immobiline (the conventional *ca.* 10 m*M* buffering ion) we are in fact increasing the charge density on the polymer coil and this results in sharper protein zones and increased protein loading capacity (see Section 5.2); (b) below 3% T, the viscoelastic forces of the gel are weakened, allowing the osmotic forces in the protein zone to take over and draw more water from surrounding gel regions; this results in a further increment in load ability within a given protein zone. Taking advantage of these findings, we have been able to load in a 5 mm thick gel, 245 cm long and 110 mm wide, containing 2.8% T matrix, in a 0.8 pH unit span (pH 6.9–7.7), 1 g of total haemoglobin, maintaining full resolution between Hb A and Hb A_{1c} (ΔpI = 0.04) and confining as much as 650 mg of protein into the main Hb A band. How we could possibly load so much protein is shown in the altimetric profile in Fig. 38: within the main Hb A zone so much water is drawn that the gel swells to an almost double thickness so that the protein has a much higher transverse gel section to dissolve in than the original 5 mm gel thickness. With this, I believe we are entering a new era in separation techniques because, for the first time, we are able to grasp both horns of the

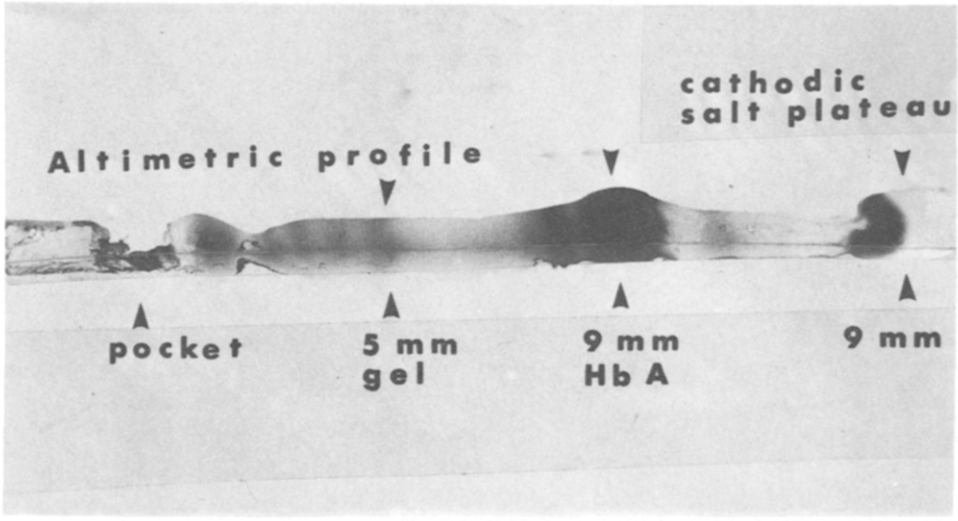

Fig. 38. Altimetric profile of a 5 mm thick, 245 mm long and 110 mm wide IPG gel loaded with 1 g of total Hb in a pH 6.9 7.9 gradient containing 2.8% T. A transverse section, parallel to the voltage and pH gradient, was cut from the short side of this gel. It shows the considerably swollen Hb A zone and the cathodic salt plateau, with the curled Hb A_2 zone. Notice how a good separation is maintained in all the protein zones even throughout the gel thickness. On the lower gel side the plastic backing of the Gel Bond PAG film can be seen (from Righetti and Gelfi; see ref. 20).

dilemma, how to load large amounts of protein in the preparative scale while still maintaining the resolution obtained in analytical runs.

6. ARTEFACTS: ASKING THE IMPOSSIBLE

When describing a new technique, it is important to define the limits of its validity, within which the method behaves as predicted. Outside these borders, the method could give erroneous answers likely to lead to misinterpretation of experimental data. For instance, in conventional IEF in presence of amphoteric buffers, several types of artefacts have been reported: binding of carrier ampholytes to nucleic acids[56], to heparin[57,58], to polyanions[59] and even to dyes[60]. This complex formation resulted in a multi-modal sample distribution (with heparin, more than 20 zones with different p*I*s in the pH interval 3.5–4.5) representing the complex between the same type of macromolecule and different types of carrier ampholytes, with different p*I* values. The IPG technique is no exception to this rule, although artefacts will occur by a different mechanism: as the charge density of the macromolecule to be separated approaches the charge density of the matrix, a strong interaction will occur, which will result either in total sample precipitation at the application point, or in extended smears covering a wide gel surface. We have found that IPG matrices interact strongly with at least two classes of proteins, histones and the histone-like, "high-mobility group" (HMG) chromatin proteins, forming insoluble complexes. The nature of these interactions has been demonstrated to be purely ionic: the complexes are split by high ionic strength (0.5 *M* sodium chloride) and/or by altering the pH (full disaggregation being obtained at pH 5.5 and 11.5). By preparing soluble homo-Immobiline polymers (polymerized in the absence of a cross-linker) formed either by a pure carboxyl or by a pure amino surface, we have demonstrated[61] that histones and HMGs bind preferentially with "carboxyl" Immobiline polymers (see Fig. 39). Thus,

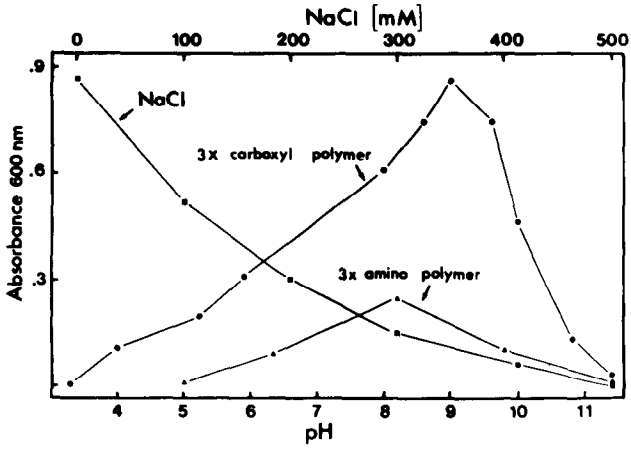

Fig. 39. Formation and disaggregation of complexes between soluble, carboxyl and amino Immobilines and histone-like (HMG) proteins. Polymers with pure carboxyl or amino surfaces, having a 3-fold higher concentration of Immobilines than standard gels (*ca.* 30 m*M*), were used in this experiment, and the stability of their complexes with HMG proteins was studied as a function of pH. With the carboxyl polymer, the disaggregation of its HMG protein complex by increasing sodium chloride molarities is also plotted (from Righetti *et al.*; see ref. 61).

one should not ask the impossible of the IPG technique: nucleic acids, heparin and polyanions also will not be amenable to fractionation in IPG matrices, and will produce a curtain of molecules smeared over the gel surface or simply precipitated at the application point. Except for these limitations, we have found that IPGs perform normally with all the proteins we have tried (having p*I*s in the pH range 3.5–10) except one: serum albumin (HSA). As seen in the separations of Görg *et al.*[62] and Cleve *et al.*[63], HSA produces long smears between pH 4.7 and 5.2, instead of focusing regularly. We believe that HSA recognizes as ligands p*K* 4.4 and 4.6 Immobilines, which are unfortunately needed as buffers in the pH region in which HSA is isoelectric. These complexes are, however, sensitive to 8 *M* urea, so that practically normal patterns are obtained when running 2-D maps by the O'Farrell technique (Gianazza and Righetti, to be published).

7. CONCLUSION NO. 1: WHERE DO WE STAND?

There are a host of electrophoretic techniques available today, of which four are the basic variants: zone electrophoresis (ZE), moving boundary electrophoresis (MBE), isotachophoresis (ITP) and isoelectric focusing (IEF). In this system, what are the coordinates of our new IPG technique? I started to elaborate complex answers, when I found that Bier *et al.*[64] had already solved the problem. They have described a mathematical model, constructed from the fundamental equations of

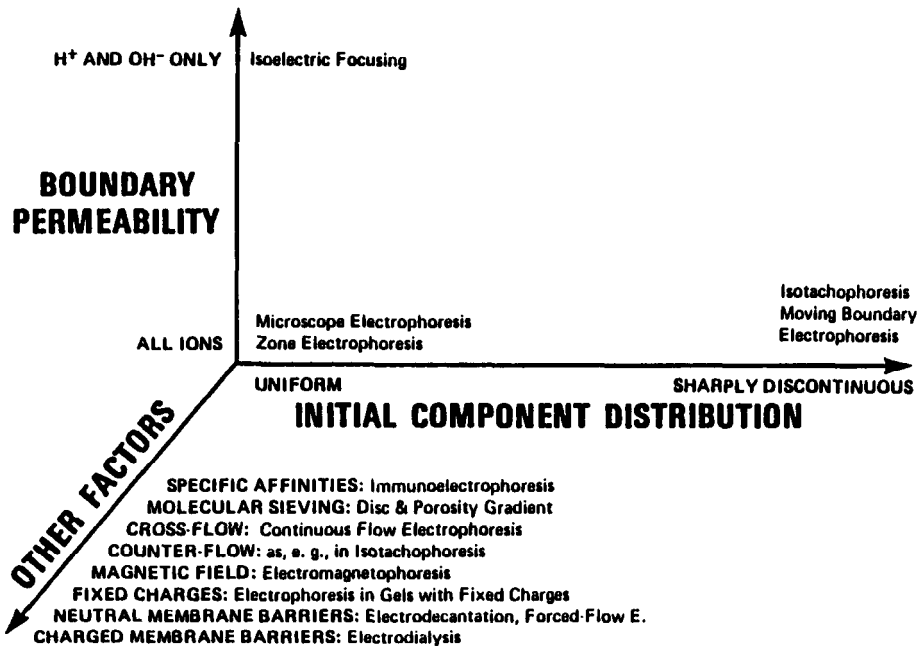

Fig. 40. Schematic representation of the four basic electrophoretic techniques and their possible relationships. The four fundamental electrophoretic processes (ZE, MBE, ITP and IEF) are seen lying on an *x*–*y* plane defined as the "Hittorf-Kohlrausch" space. Several additional constraints are distributed along the *z*-axis: IPGs can be found on the upper *y*-axis (isoelectric focusing) and on the *z*-axis (fixed charges) (from Dr. Milan Bier, deleted from a paper in *Science*; see ref. 64).

mass transport, dissociation equilibria, conservation of mass and charge and the principle of electroneutrality, which applies to all the different electrophoretic processes. To put it in their own words: "It is important to note that ZE, MBE, ITP and IEF differ only in the initial distribution of components along the electrophoretic column and the boundary permeability —stipulations that can be traced to Kohlrausch[65] and Hittorf[66]. The Kohlrausch–Hittorf constraints can be seen as defining an "electrophoretic plane", wherein these four modes represent idealized points within a virtually infinite gradation of possibilities". How we can visualize this plane is shown in Fig. 40; I should like to focus your attention on this graph, which is offered to you as a "world première"; it was given to me by my friend Milan Bier and it was meant to belong to his paper in Science[64]. Unfortunately, some nincompoop sub-sub-desk editor exerted a strong censorship on it and deleted the most juicy part of it. The Hittorf–Kohlrausch "electrophoretic space", defined by the x–y plane, is implemented by a z-axis carrying all the constraints not considered originally, such as specific affinities (immunoelectrophoresis), molecular sieving (pore gradient gels), cross-flow (continuous-flow electrophoresis), counter-flow (as occasionally utilized in ITP), magnetic fields (as in electromagnetophoresis), fixed charges (and here Bier *et al.* have spotted us: IEF in IPGs). Hence the coordinates of our system can be found in a curved surface cutting high up across the boundary permeability axis and at the fixed charges level in the "other factors", z-axis.

8. CONCLUSION NO. 2: "THE PHILOSOPHER'S STONE"

After reading about all the wonders of IPGs you might have the impression of having found the philosopher's stone, the magic one that transmutes metals into gold. Let me end with a note of caution: not always can this stone bring you happiness, as you will see in this story which I heard from my friend François-Marie Arouet[67].

"Deux Italiens, dont l'un s'appelait Exili, travaillèrent longtemps avec un apothicaire allemand, nommé Glaser, à rechercher ce qu'on appelle la pierre philosophale. Les deux italiens y perdirent le peu qu'ils avaient, et voulurent, par le crime, réparer le tort de leur folie; ils vendirent secrètement des poisons. La confession, le plus grand frein de la méchanceté humaine, mais dont on abuse en croyant pouvoir faire des crimes qu'on croit expier; la confession, dis-je, fit connaître au grand pénitencier de Paris que quelques personnes étaient mortes empoisonnées. Il en donna avis au gouvernement. Les deux Italiens soupçonnés furent mis à la Bastille: l'un des deux y mourut. Exili y resta sans être convaincu; et, du fond de sa prison, il répandit dans Paris ces funestes secrets qui coutèrent la vie au lieutenant civil d'Aubral et à sa famille, et qui firent enfin ériger la chambre des poisons, qu'on nomme la chambre ardente".

As I do not want to end up in the Bastille, or in the "chambre ardente", I suggest you take the IPG technique just for what it is: a very powerful fractionation technique, possibly the most advanced of all electrophoretic methods, potentially able to solve many biological problems, definitely unable to transmute your lead shield into gold.

9. ACKNOWLEDGEMENTS

P.G.R. is supported by a 5-year grant from Consiglio Nazionale delle Ricerche (CNR, Rome, Italy), Progetto Finalizzato "Salute dell'Uomo", Sottoprogetto "Meccanismi di Invecchiamento", for the development of 2-D maps with "IPG-DALT" coordinates. I hope you have enjoyed this "Italian Graffiti", even though I am sure you are more familiar with the movie "American Graffiti". Many the cast members: Drs. B. Bjellqvist, E. Gianazza, A. Görg, R. Westermeier, C. Gelfi and G. Dossi and Profs. F. Celentano and W. Postel. The Milan–Munich–Bromma collaboration was exciting, ambitious, hard and excruciating, at times, but always full of life and understanding. The team has now dissolved and unfortunately some of them will never be back (we have lost our dearest friend Giulio Dossi in a motorbike accident), but beware! —like in the paintings of Rousseau (Le Douanier), the fauves, hidden in the jungle, are watching you with beady, yellow eyes.

10. SUMMARY

The state of the art in the new technique of isoelectric focusing (IEF) in immobilized pH gradients (IPG) is extensively reviewed. The first section details the theory of the formation of narrow and ultra-narrow pH gradients on the tandem principle (one buffer, one titrant) as well as the computer program and algorithms for the generation of extended pH intervals (>2 pH units). The second section is entirely devoted to the methodological aspects of IPGs: from gel casting, to polymerization kinetics and to the use of additives and pH plateaux for salt removal. The third section deals in depth with preparative aspects of IPGs, especially with regard to the optimization of environmental parameters (ionic strength, gel thickness and width of the pH gradient interval). Methods of protein detection, electrophoretic retrieval into hydroxyapatite beads, elution from Ultrogel grains and protein load as a function of polyacrylamide gel concentration are critically evaluated. The review ends with a section on the merits and limits of IPGs, possible sources of artefacts, their interpretation and possible future uses of the IPG technique.

REFERENCES

1 E. A. Poe, *Selected Writings*, Penguin Books, Harmondsworth, 1967, pp. 127–137.
2 A. Kolin, *Methods Biochem. Anal.*, 6 (1958) 259–288.
3 H. Svensson, *Acta Chem. Scand.*, 15 (1961) 325–341; 16 (1962) 456–466.
4 B. Bjellqvist, K. Ek, P. G. Righetti, E. Gianazza, A. Görg, W. Postel and R. Westermeier, *J. Biochem. Biophys. Methods*, 6 (1982) 317–339.
5 P. G. Righetti and J. W. Drysdale, *Ann. N.Y. Acad. Sci.*, 209 (1973) 163–186.
6 P. G. Righetti and J. W. Drysdale, *J. Chromatogr.*, 98 (1974) 271–321.
7 P. G. Righetti, *J. Chromatogr.*, 190 (1980) 275–282.
8 P. G. Righetti, *Isoelectric Focusing: Theory, Methodology and Applications*, Elsevier, Amsterdam, 1983, pp. 268–273.
9 J. Porath, R. Axen and S. Ernback, *Nature (London)*, 215 (1967) 1491–1493.
10 P. Cuatrecasas, *Advan. Enzymol.*, 36 (1972) 29–40.
11 L. B. Wingard, Jr., E. Katchalski-Katzir and L. Goldstein (Editors), *Applied Biochemistry and Bioengineering*, Vol. 3, 1981; I. Chibata and L. B. Wingard, Jr. (Editors), *Applied Biochemistry and Bioengineering*, Vol. 4, 1983; Academic Press, New York.

12 A. Kolin, in B. J. Radola and D. Graesslin (Editors), *Isoelectric Focusing and Isotachophoresis*, Walter de Gruyter, Berlin, 1977, pp. 3–33.
13 A. J. P. Martin and F. Hampson, *J. Chromatogr.*, 159 (1978) 101–110.
14 H. Rilbe, *J. Chromatogr.*, 159 (1978) 193–205.
15 Y. Matuo, J. Horio, H. Saito, Y. Suzuki and F. Yanai, *Prot. Nucl. Acids Enzyme*, 9 (1978) 13–28.
16 P. G. Righetti, E. Gianazza and B. Bjellqvist, *J. Biochem. Biophys. Methods*, 8 (1983) 89–108.
17 S. Fredriksson, in B. J. Radola and D. Graesslin (Editors), *Isoelectric Focusing and Isotachophoresis*, Walter de Gruyter, Berlin, 1977, pp. 71–83.
18 E. Gianazza, F. Chillemi, M. Duranti and P. G. Righetti, *J. Biochem. Biophys. Methods*, 8 (1983) 339–351.
19 C. Gelfi and P. G. Righetti, *Electrophoresis*, 2 (1981) 220–228.
20 P. G. Righetti and C. Gelfi, *J. Biochem. Biophys. Methods*, 9 (1984) in press.
21 P. O'Farrell, *J. Biol. Chem.*, 250 (1975) 4007–4021.
22 J. Rochette, P. G. Righetti, A. Bianchi Bosisio, F. Vertogen, G. Schneck, J. P. Boissel, D. Labie and H. Wajcman, *J. Chromatogr.*, 285 (1984) 143–152.
23 J. W. Drysdale, P. G. Righetti and H. F. Bunn, *Biochim. Biophys. Acta*, 229 (1971) 42–53.
24 G. Dossi, F. Celentano, E. Gianazza and P. G. Righetti, *J. Biochem. Biophys. Methods*, 7 (1983) 123–142.
25 E. Gianazza, G. Dossi, F. Celentano and P. G. Righetti, *J. Biochem. Biophys. Methods*, 8 (1983) 109–133.
26 P. G. Righetti, E. Gianazza, G. Dossi, F. Celentano, B. Bjellqvist, K. Ek, B. Sahlin and C. Eklund, in H. Hirai (Editor), *Electrophoresis '83*, Walter de Gruyter, Berlin, 1983, in press.
27 P. E. Nute, G. Stamatoyannopoulos, M. A. Hermodson and D. Roth, *J. Clin. Invest.*, 53 (1974) 320–328.
28 H. Rilbe, *Ann. N.Y. Acad. Sci.*, 209 (1973) 11–22.
29 O. Vesterberg and H. Svensson, *Acta Chem. Scand.*, 20 (1966) 820–834.
30 L. Ornstein, *Ann. N.Y. Acad. Sci.*, 121 (1964) 321–349.
31 E. A. Peterson and H. A. Sober, *Anal. Chem.*, 31 (1959) 857–862.
32 P. Debye and E. Hückel, *Physik. Z.*, 24 (1924) 305–330.
33 C. Gelfi and P. G. Righetti, *J. Biochem. Biophys. Methods*, 8 (1983) 157–172.
34 H. Delincée and B. J. Radola, *Anal. Biochem.*, 90 (1978) 609–623.
35 P. Burdett, *Isoelectric Focusing, Principles and Methods*, Pharmacia, Uppsala, 1982, pp. 31–36.
36 P. G. Righetti, G. Tudor and E. Gianazza, *J. Biochem. Biophys. Methods*, 6 (1982) 219–227.
37 J. M. Gershoni and G. E. Palade, *Anal. Biochem.*, 131 (1983) 1–15.
38 A. Görg, W. Postel and R. Westermeier, *Anal. Biochem.*, 89 (1978) 60–70.
39 P. J. Flory, *Principles of Polymer Chemistry*, Cornell University Press, Ithaca, NY, 1953.
40 S. L. Aggarwal, *Polymer*, 17 (1976) 38–956.
41 F. Danusso, G. Tieghi and T. Ricco, *Polymer*, 20 (1979) 805–812.
42 C. Gelfi and P. G. Righetti, *Electrophoresis*, 2 (1981) 213–219.
43 P. G. Righetti, C. Gelfi and A. Bianchi Bosisio, *Electrophoresis*, 2 (1981) 291–295.
44 E. Gianazza, G. Artoni and P. G. Righetti, *Electrophoresis*, 4 (1983) 321–326.
45 E. Gianazza, C. Astorri and P. G. Righetti, *J. Chromatogr.*, 171 (1979) 161–169.
46 M. Jonsson, *Electrophoresis*, 1 (1980) 141–149.
47 K. Ek, B. Bjellqvist and P. G. Righetti, *J. Biochem. Biophys. Methods*, 8 (1983) 135–155.
48 P. G. Righetti, *Trends Anal. Chem.*, 2 (1983) 193–196.
49 J. E. Cohn, *Chem. Rev.*, 19 (1936) 241–255.
50 A. Gronwall, *C.R. Trav. Lab. Carlsberg, Ser. Chim.*, 24 (1942) 185–195.
51 P. G. Righetti, M. Pagani and E. Gianazza, *J. Chromatogr.*, 109 (1975) 341–356.
52 B. R. Ziola and D. G. Scraba, *Anal. Biochem.*, 72 (1976) 366–371.
53 J. Guevara, Jr., E. A. Chiocca, L. F. Clayton, A. L. von Eschenback and J. J. Edwards, *Clin. Chem.*, 28 (1982) 756–758.
54 B. J. Radola, *Biochim. Biophys. Acta*, 386 (1974) 181–195.
55 S. Hjertén, in N. Catsimpoolas (Editor), *Methods of Protein Separation*, Vol. 2, Plenum Press, New York, 1976, pp. 233–243.
56 E. Galante, T. Caravaggio and P. G. Righetti, *Biochim. Biophys. Acta*, 442 (1976) 309–315.
57 P. G. Righetti and E. Gianazza, *Biochim. Biophys. Acta*, 532 (1978) 137–146.
58 P. G. Righetti, R. P. Brown and A. L. Stone, *Biochim. Biophys. Acta*, 542 (1978) 232–244.